Membership-Mappings for Practical Secure Distributed Deep Learning

Mohit Kumar, Weiping Zhang, Lukas Fischer, and Bernhard Freudenthaler

Abstract—**This study leverages the data representation capability of fuzzy based membership-mappings for practical secure distributed deep learning using fully homomorphic encryption. The impracticality issue of secure machine (deep) learning with fully homomorphic encrypted data, arising from large computational overhead, is addressed via applying fuzzy attributes. Fuzzy attributes are induced by globally convergent and robust variational membership-mappings based local deep models. Fuzzy attributes combine the local deep models in a robust and flexible manner such that the global model can be evaluated homomorphically in an efficient manner using a boolean circuit composed of bootstrapped binary gates. The proposed method, while preserving privacy in a distributed learning scenario, remains accurate, practical, and scalable. The method is evaluated through numerous experiments including demonstrations through MNIST dataset and Freiburg Groceries Dataset. Further, a biomedical application related to mental stress detection on individuals is considered.**

Index Terms—**Membership-mappings, fully homomorphic encryption, fuzzy attributes, distributed deep learning, privacy.**

I. INTRODUCTION

FULLY homomorphic encryption (FHE) is a solution to the privacy concerns in the cloud computing scenario. The first FHE scheme [1] is based on ideal lattices and the bootstrapping procedure is introduced to reduce the noise contained in a ciphertext for allowing arbitrary computations. The bootstrapping operation is performed on a ciphertext via evaluating the decryption function homomorphically using the bootstrapping key (which is the encryption of the private decryption key under the public encryption key). Bootstrapping is the computationally most expensive part of a homomorphic encryption scheme. The theoretical breakthrough of [1] was followed by several attempts to develop more practical FHE schemes. The scheme introduced in [2] uses only elementary modulo arithmetic and is homomorphic with regard to both addition and multiplication. This scheme was improved in

M. Kumar is with the Software Competence Center Hagenberg, Austria and the Faculty of Computer Science and Electrical Engineering, University of Rostock, Germany.

W. Zhang is with the Northwestern Polytechnical University, Suzhouzhong Road, Suzhou, China, e-mail: zhangweiping@zjubh.com.

L. Fischer and B. Freudenthaler are with the Software Competence Center Hagenberg, Austria.

[3] with reduced public key size, extended in [4] to support encrypting and homomorphically processing a vector of plaintexts as a single ciphertext, and generalized to non-binary messages in [5]. Schemes based on a different hard problem, referred to as Learning With Errors (LWE) problem [6], were constructed and many current schemes still rely on LWE or its variants. A FHE scheme constructed in [7] is based solely on the standard LWE assumption that is known to be at least as hard as solving hard problems in general lattices. In a variant of the LWE problem, called ring learning with errors problem (RLWE) problem, the algebraic structure of the underlying hard problem reduces the key sizes and speeds up the homomorphic operations. A leveled fully homomorphic encryption scheme based on LWE or RLWE, without bootstrapping procedure, was proposed in [8]. The ciphertexts contain a certain amount of noise for security purposes that grows with homomorphic operations. For a better management of the noise growth, [8] introduced a modulus switching technique where a complete ladder of moduli is used for scaling down the ciphertext to the next modulus after each multiplication. A tensoring technique for LWE-based FHE that reduced ciphertext noise growth after multiplication from quadratic to linear was introduced in [9]. As the scheme of [9] does no longer require the rescaling of the ciphertext, this scheme was called a scale-invariant fully homomorphic encryption scheme. An RLWE version of the scale-invariant scheme of [9] was created in [10]. A technique for building LWE based FHE scheme called as approximate eigenvector method in which homomorphic addition and multiplication are just matrix addition and multiplication was proposed in [11]. The essence of this scheme is that the secret key is an approximate eigenvector of the ciphertext matrix and the message is the corresponding eigenvalue. Several works that followed the theoretical breakthrough of [1] were aimed at improving the bootstrapping as the bootstrapping remained the bottleneck for an efficient FHE in practice. A much faster bootstrapping, based on a scheme similar to the type of [11] that allows to homomorphically compute simple bit operations and refresh (bootstrap) the resulting output in less than a second, was devised in [12]. Finally, the TFHE scheme was proposed in [13], [14] that features an improved bootstrapping procedure that is considerably more efficient than the previous state of the art. The TFHE scheme generalizes previous structures and schemes over the torus (i.e., the reals modulo 1) and improves the bootstrapping dramatically. For practical applications, TFHE is an open-source C/C++ library [15] implementing the ring-variant of [11] together with the optimizations of [12]–[14]. TFHE library implements a very

fast gate-by-gate bootstrapping and supports the homomorphic evaluation of the binary gates. The library allows to evaluate homomorphically an arbitrary boolean circuit composed of binary gates without restriction on the number of gates or on their composition, over encrypted data, without decrypting. However, the bootstrapped bit operations are still several times slower than their plaintext equivalents.

The fuzzy systems' capability of handling uncertainties in a rigorous mathematical manner has motivated combining fuzzy theory with deep models [16]–[20], [20]–[23]. Deep neural networks outperform classical machine learning techniques in a wide range of applications but their training requires a large amount of data. The issues, such as determining the optimal model structure, requirement of large training dataset, and iterative time-consuming nature of numerical learning algorithms, are inherent to the neural networks based parametric deep models. The nonparametric approach on the other hand can be promising to address the issue of optimal choice of model structure. However, an analytical solution instead of iterative gradient-based numerical algorithms will be still desired for the learning of deep models. These motivations have led to the development of a nonparametric deep model [24]–[26] that is learned analytically for representing data points. The study in [24]–[26] introduces the concept of fuzzy-mapping which is about representing mappings through a fuzzy set such that the dimension of membership function increases with an increasing data size. A relevant result is that a deep autoencoder model formed via a composition of finite number of nonparametric fuzzy-mappings can be learned analytically via variational optimization technique. However, [24]–[26] didn't provide a formal mathematical framework for the conceptualization of so-called fuzzy-mapping. The study in [27] provides to fuzzy-mapping a measure-theoretic conceptualization and refers it to as *membership-mapping*. Further, the membership-mapping could serve as the building block of deep models [28]. An alternative idea of deep autoencoder, that consists of layers such that each layer learns data representation at certain abstraction level through a membership-mappings based autoencoder, is introduced in [28] for data representation learning.

The aim of this study is to develop a methodology for practical secure distributed deep learning using fully homomorphic encryption. The machine (deep) learning with fully homomorphically encrypted data remains impractical due to the large computational overhead. Thus, we address in this study the impracticality issue of secure distributed deep learning via

1) leveraging data representation learning capability of globally convergent and robust membership-mappings to build local deep models,
2) using local deep models to induce fuzzy attributes such that defined fuzzy attributes learn data representation,
3) combining local deep models in a robust and flexible manner by means of fuzzy attributes and fuzzy rules to define a global model,
4) defining the global model in such a way that the global model can be evaluated homomorphically in an efficient manner using a boolean circuit composed of bootstrapped binary gates,

5) implementing very fast gate-by-gate bootstrapping to homomorphically evaluate the global model (that combines the distributed local models) to predict the output.

The proposed approach to secure distributed deep learning is novel. To the best knowledge of the authors, this is the first study to apply fuzzy attributes, which are induced by globally convergent and robust variational membership-mappings based local deep models, for an efficient homomorphic evaluation of the global model. The idea of using fuzzy sets and fuzzy rules to aggregate the local private deep models for building the global model was also considered in [29], however, under differential privacy framework. Differential privacy preserves the privacy of the training dataset via adding random noise to ensure that an adversary can not infer any single data instance by observing model parameters or model outputs. The amount of noise depends upon the value of privacy-loss bound. A major limitation of the differential privacy is that a sufficiently low value of privacy-loss bound results in a loss of accuracy. Moreover, it is not clear how to practically choose the value of privacy-loss bound. FHE approach on the other hand does not lead to the loss of accuracy, however, requires a large computational time.

The data representation learning capability of membership-mappings is central to our methodology. Although [27] provided an algorithm for the variational learning of membership-mappings via following the approach of [24]–[26], there remains the following two limitations:

1) there is no mathematical proof regarding the convergence of the learning algorithm, and
2) there is no mathematical analysis on the robustness of the learning algorithm.

This study addresses these two limitations and presents a more simple and elegant estimation algorithm for the variational learning of membership-mappings. A convergence analysis is carried out via deriving a sufficient condition for the convergence of the estimation algorithm. The convergence analysis allows to provide a globally convergent algorithm for the variational learning of membership-mappings based deep models. Further, it is shown that the learning algorithm provides a robust estimation of model parameters via solving a min-max estimation problem. The proposed method for secure distributed deep learning is implemented using MAT-LAB R2017b and TFHE C/C++ library [15]. Experiments have been performed to evaluate the method (in-terms of accuracy and computational time) on MNIST dataset, Freiburg Groceries Dataset, and a biomedical dataset consisting of heart rate interval measurements of different subjects. Further, the scalability of the method as the number of parties participating in collaborative learning increases is investigated.

The paper is organized into sections. Section II reviews the membership-mappings from previous works. An estimation algorithm for the variational learning of membership-mappings is provided in Section III. The convergence and robustness issues have been addressed in Section IV. Section V considers the application of membership-mappings to the secure distributed deep learning problem. The experimental validation of the method is provided in Section VI. Finally, the concluding

remarks are stated in Section VII.

II. REVIEW OF MEMBERSHIP-MAPPINGS

This section is dedicated to the review of variational membership-mappings from previous works [27], [28].

A. Notations and Definitions

- Let $n, N, p, M \in \mathbb{N}$.
- Let $\mathcal{B}(\mathbb{R}^N)$ denote the *Borel $\sigma-algebra$* on $\mathbb{R}^N$, and let λ^N denote the *Lebesgue measure* on $\mathcal{B}(\mathbb{R}^N)$.
- Let $(\mathcal{X}, \mathcal{A}, \rho)$ be a probability space with unknown probability measure ρ.
- Let us denote by $\mathcal{S}$ the set of finite samples of data points drawn i.i.d. from ρ, i.e.,

$$\mathcal{S} := \{(x^i \sim \rho)_{i=1}^N \mid N \in \mathbb{N}\}. \qquad (1)$$

- For a sequence $\mathrm{x} = (x^1, \cdots, x^N) \in \mathcal{S}$, let $|\mathrm{x}|$ denote the cardinality i.e. $|\mathrm{x}| = N$.
- If $\mathrm{x} = (x^1, \cdots, x^N)$, $\mathrm{a} = (a^1, \cdots, a^M) \in \mathcal{S}$, then $\mathrm{x} \wedge \mathrm{a}$ denotes the concatenation of the sequences x and a, i.e., $\mathrm{x} \wedge \mathrm{a} = (x^1, \ldots, x^N, a^1, \ldots, a^M)$.
- Let us denote by $\mathbb{F}(\mathcal{X})$ the set of $\mathcal{A}$-$\mathcal{B}(\mathbb{R})$ measurable functions $f : \mathcal{X} \to \mathbb{R}$, i.e.,

$$\mathbb{F}(\mathcal{X}) := \{f : \mathcal{X} \to \mathbb{R} \mid f \text{ is } \mathcal{A}\text{-}\mathcal{B}(\mathbb{R}) \text{ measurable}\}. (2)$$

- For convenience, the values of a function $f \in \mathbb{F}(\mathcal{X})$ at points in the collection $\mathrm{x} = (x^1, \cdots, x^N)$ are represented as $f(\mathrm{x}) = (f(x^1), \cdots, f(x^N))$.
- Given two $\mathcal{B}(\mathbb{R}^N) - \mathcal{B}(\mathbb{R})$ measurable mappings, $g : \mathbb{R}^N \to \mathbb{R}$ and $\mu : \mathbb{R}^N \to \mathbb{R}$, the weighted average of $g(\mathrm{y})$ over all $\mathrm{y} \in \mathbb{R}^N$, with $\mu(\mathrm{y})$ as the weighting function, is computed as

$$\langle g \rangle_\mu := \frac{1}{\int_{\mathbb{R}^N} \mu(\mathrm{y}) \, \mathrm{d}\lambda^N(\mathrm{y})} \int_{\mathbb{R}^N} g(\mathrm{y})\mu(\mathrm{y}) \, \mathrm{d}\lambda^N(\mathrm{y}). \quad (3)$$

- For a sequence $\mathrm{x} \in \mathcal{S}$, assume that a membership function $\zeta_\mathrm{x} : \mathbb{R}^{|\mathrm{x}|} \to [0, 1]$ satisfies the following properties:
  - $\zeta_\mathrm{x}(\mathrm{y}) > 0$ for all $\mathrm{y} \in \mathbb{R}^{|\mathrm{x}|}$, i.e.,

$$\mathrm{supp}[\zeta_\mathrm{x}] = \mathbb{R}^{|\mathrm{x}|}. \qquad (4)$$

  - the functions ζ_x are absolutely continuous and Lebesgue integrable over the whole domain such that for all $\mathrm{x} \in \mathcal{S}$ we have

$$0 < \int_{\mathbb{R}^{|\mathrm{x}|}} \zeta_\mathrm{x} \, \mathrm{d}\lambda^{|\mathrm{x}|} < \infty. \qquad (5)$$

  - the membership function induced probability measures $\mathbb{P}_{\zeta_\mathrm{x}}$, defined on any $A \in \mathcal{B}(\mathbb{R}^{|\mathrm{x}|})$, as

$$\mathbb{P}_{\zeta_\mathrm{x}}(A) := \frac{1}{\int_{\mathbb{R}^{|\mathrm{x}|}} \zeta_\mathrm{x} \, \mathrm{d}\lambda^{|\mathrm{x}|}} \int_A \zeta_\mathrm{x} \, \mathrm{d}\lambda^{|\mathrm{x}|} \qquad (6)$$

  are consistent in the sense that for all x, a $\in \mathcal{S}$:

$$\mathbb{P}_{\zeta_{\mathrm{x} \wedge \mathrm{a}}}(A \times \mathbb{R}^{|\mathrm{a}|}) = \mathbb{P}_{\zeta_\mathrm{x}}(A). \qquad (7)$$

The collection of membership functions satisfying aforementioned assumptions is denoted by

$$\Theta := \{\zeta_\mathrm{x} : \mathbb{R}^{|\mathrm{x}|} \to [0, 1] \mid (4), (5), (7), \ \mathrm{x} \in \mathcal{S}\}. \quad (8)$$

Definition 1 (Student-t Membership-Mapping [27]): A Student-t membership-mapping, $\mathcal{F} \in \mathbb{F}(\mathcal{X})$, is a mapping with input space $\mathcal{X} = \mathbb{R}^n$ and a membership function $\zeta_\mathrm{x} \in \Theta$ that is Student-t like:

$$\zeta_\mathrm{x}(\mathrm{y}) = \left(1 + \frac{1}{\nu - 2} (\mathrm{y} - \mathrm{m_y})^T K_{\mathrm{xx}}^{-1} (\mathrm{y} - \mathrm{m_y})\right)^{-\frac{\nu + |\mathrm{x}|}{2}} \quad (9)$$

where $\mathrm{x} \in \mathcal{S}$, $\mathrm{y} \in \mathbb{R}^{|\mathrm{x}|}$, $\nu \in \mathbb{R}_+ \setminus [0, 2]$ is the degrees of freedom, $\mathrm{m_y} \in \mathbb{R}^{|\mathrm{x}|}$ is the mean vector, and $K_{\mathrm{xx}} \in \mathbb{R}^{|\mathrm{x}| \times |\mathrm{x}|}$ is the covariance matrix with its $(i, j)-$th element given as

$$(K_{\mathrm{xx}})_{i,j} = kr(x^i, x^j) \qquad (10)$$

where $kr : \mathbb{R}^n \times \mathbb{R}^n \to \mathbb{R}$ is a positive definite kernel function defined as

$$kr(x^i, x^j) = \sigma^2 \exp\left(-0.5 \sum_{k=1}^n w_k \left|x_k^i - x_k^j\right|^2\right) \quad (11)$$

where x_k^i is the $k-$th element of x^i, σ^2 is the variance parameter, and $w_k \geq 0$ (for $k \in \{1, \cdots, n\}$).

B. Conditionally Deep Autoencoders

This subsection reviews the conditionally deep models [28] formed by the compositions of membership-mappings.

Definition 2 (Membership-Mapping Autoencoder [28]): A membership-mapping autoencoder, $\mathcal{G} : \mathbb{R}^p \to \mathbb{R}^p$, maps an input vector $y \in \mathbb{R}^p$ to $\mathcal{G}(y) \in \mathbb{R}^p$ such that

$$\mathcal{G}(y) \stackrel{\text{def}}{=} [\mathcal{F}_1(Py) \ \cdots \ \mathcal{F}_p(Py)]^T, \qquad (12)$$

where $\mathcal{F}_j$ $(j \in \{1, 2, \cdots, p\})$ is a Student-t membership-mapping, $P \in \mathbb{R}^{n \times p}(n \leq p)$ is a matrix such that the product Py is a lower-dimensional encoding for y.

Definition 3 (Conditionally Deep Membership-Mapping Autoencoder (CDMMA) [28]): A conditionally deep membership-mapping autoencoder, $\mathcal{D} : \mathbb{R}^p \to \mathbb{R}^p$, maps a vector $y \in \mathbb{R}^p$ to $\mathcal{D}(y) \in \mathbb{R}^p$ through a nested composition of finite number of membership-mapping autoencoders such that

$$y^l = (\mathcal{G}_l \circ \cdots \circ \mathcal{G}_2 \circ \mathcal{G}_1)(y), \ \forall l \in \{1, 2, \cdots, L\} \quad (13)$$

$$l^* = \arg \min_{l \in \{1, 2, \cdots, L\}} \|y - y^l\|^2 \qquad (14)$$

$$\mathcal{D}(y) = y^{l^*}, \qquad (15)$$

where $\mathcal{G}_l(\cdot)$ is a membership-mapping autoencoder (Definition 2).

Definition 4 (A Wide CDMMA [28]): A wide CDMMA, $\mathcal{WD} : \mathbb{R}^p \to \mathbb{R}^p$, maps a vector $y \in \mathbb{R}^p$ to $\mathcal{WD}(y) \in \mathbb{R}^p$ through a parallel composition of S ($S \in \mathcal{Z}_+$) number of CDMMAs such that

$$\mathcal{WD}(y) = \mathcal{D}_{s^*}(y) \qquad (16)$$

$$s^* = \arg \min_{s \in \{1, 2, \cdots, S\}} \|y - \mathcal{D}_s(y)\|^2, \qquad (17)$$

where $\mathcal{D}_s(y)$ is the output of $s-$th CDMMA.

III. Variational Learning of Membership-Mappings

A. A Modeling Scenario

Given a dataset $\{(x^i, y^i) \mid x^i \in \mathbb{R}^n, \ y^i \in \mathbb{R}^p, \ i \in \{1, \cdots, N\}\}$, it is assumed that there exist zero-mean Student-t membership-mappings $\mathcal{F}_1, \cdots, \mathcal{F}_p \in \mathbb{F}(\mathbb{R}^n)$ such that

$$y^i \approx \begin{bmatrix} \mathcal{F}_1(x^i) & \cdots & \mathcal{F}_p(x^i) \end{bmatrix}^T. \tag{18}$$

For $j \in \{1, 2, \cdots, p\}$, define

$$\mathrm{y}_j = \begin{bmatrix} y_j^1 & \cdots & y_j^N \end{bmatrix}^T \in \mathbb{R}^N \tag{19}$$

$$\mathrm{f}_j = \begin{bmatrix} \mathcal{F}_j(x^1) & \cdots & \mathcal{F}_j(x^N) \end{bmatrix}^T \in \mathbb{R}^N \tag{20}$$

where y_j^i denotes the $j-$th element of y^i. A set of auxiliary inducing points, $\mathrm{a} = \{a^m \in \mathbb{R}^n \mid m \in \{1, \cdots, M\}\}$, is introduced to define

$$\mathrm{u}_j = \begin{bmatrix} \mathcal{F}_j(a^1) & \cdots & \mathcal{F}_j(a^M) \end{bmatrix}^T \in \mathbb{R}^M. \tag{21}$$

B. Membership Functional Representation Approach

Definition 5 (Interpolation Based Representation): It follows from [27] that f_j, based upon an interpolation on the auxiliary-outputs u_j, is represented by means of a membership function, $\mu_{\mathrm{f}_j;\mathrm{u}_j} : \mathbb{R}^N \to [0, 1]$, as

$$\left(\mu_{\mathrm{f}_j;\mathrm{u}_j}(\tilde{\mathrm{f}}_j) \right)^{-\frac{2}{\nu+M+N}} = 1 + \tag{22}$$

$$\frac{(\tilde{\mathrm{f}}_j - \bar{m}_{\mathrm{f}_j})^T \left(\frac{\nu + (\mathrm{u}_j)^T K_{\mathrm{aa}}^{-1} \mathrm{u}_j - 2}{\nu + M - 2} \bar{K}_{\mathrm{xx}} \right)^{-1} (\tilde{\mathrm{f}}_j - \bar{m}_{\mathrm{f}_j})}{\nu + M - 2}$$

$$\bar{m}_{\mathrm{f}_j} = K_{\mathrm{xa}} K_{\mathrm{aa}}^{-1} \mathrm{u}_j \tag{23}$$

$$\bar{K}_{\mathrm{xx}} = K_{\mathrm{xx}} - K_{\mathrm{xa}} K_{\mathrm{aa}}^{-1} K_{\mathrm{xa}}^T, \tag{24}$$

where $K_{\mathrm{aa}} \in \mathbb{R}^{M \times M}$ and $K_{\mathrm{xa}} \in \mathbb{R}^{N \times M}$ are matrices with their $(i, j)-$th elements given as

$$(K_{\mathrm{aa}})_{i,j} = kr(a^i, a^j) \tag{25}$$

$$(K_{\mathrm{xa}})_{i,j} = kr(x^i, a^j) \tag{26}$$

where $kr : \mathbb{R}^n \times \mathbb{R}^n \to \mathbb{R}$ is a positive definite kernel function defined as in (11).

Definition 6 (Representation of Data y_j for Given Mappings Output f_j): y_j, for given f_j, is represented by means of a membership function, $\mu_{\mathrm{y}_j;\mathrm{f}_j} : \mathbb{R}^N \to [0, 1]$, as

$$\mu_{\mathrm{y}_j;\mathrm{f}_j}(\tilde{\mathrm{y}}_j) = \exp\left(-0.5\beta \|\tilde{\mathrm{y}}_j - \mathrm{f}_j\|^2 \right) \tag{27}$$

where $\beta > 0$ is the precision value.

Definition 7 (Representation of Data y_j for Fixed Auxiliary-Outputs u_j): y_j, for given u_j, is represented by means of a membership function, $\mu_{\mathrm{y}_j;\mathrm{u}_j} : \mathbb{R}^N \to [0, 1]$, as

$$\mu_{\mathrm{y}_j;\mathrm{u}_j}(\tilde{\mathrm{y}}_j) \propto \exp\left(\left\langle \log(\mu_{\mathrm{y}_j;\mathrm{f}_j}(\tilde{\mathrm{y}}_j)) \right\rangle_{\mu_{\mathrm{f}_j;\mathrm{u}_j}} \right) \tag{28}$$

where $\mu_{\mathrm{y}_j;\mathrm{f}_j}$ is given by (27), $\mu_{\mathrm{f}_j;\mathrm{u}_j}$ is defined as in (22), and $< \cdot >$. is the averaging operation as defined in (3). Thus, $\mu_{\mathrm{y}_j;\mathrm{u}_j}$ is obtained from $\log(\mu_{\mathrm{y}_j;\mathrm{f}_j})$ after averaging out the variables f_j using its membership function. It can be shown that

$$\mu_{\mathrm{y}_j;\mathrm{u}_j}(\tilde{\mathrm{y}}_j) \propto \exp\left(-0.5\beta\|\tilde{\mathrm{y}}_j\|^2 + (\mathrm{u}_j)^T \hat{K}_{\mathrm{u}_j}^{-1} \hat{m}_{\mathrm{u}_j}(\tilde{\mathrm{y}}_j) \right. \tag{29}$$

$$\left. -0.5(\mathrm{u}_j)^T \hat{K}_{\mathrm{u}_j}^{-1} \mathrm{u}_j + 0.5(\mathrm{u}_j)^T K_{\mathrm{aa}}^{-1} \mathrm{u}_j + \{/(\tilde{\mathrm{y}}_j, \mathrm{u}_j)\} \right)$$

where $\hat{K}_{\mathrm{u}_j}$, $\hat{m}_{\mathrm{u}_j}(\tilde{\mathrm{y}}_j)$ are given as

$$(\hat{K}_{\mathrm{u}_j})^{-1} = K_{\mathrm{aa}}^{-1} + \beta K_{\mathrm{aa}}^{-1} K_{\mathrm{xa}}^T K_{\mathrm{xa}} K_{\mathrm{aa}}^{-1} \tag{30}$$

$$+ \beta \frac{\mathrm{tr}(K_{\mathrm{xx}} - K_{\mathrm{aa}}^{-1} K_{\mathrm{xa}}^T K_{\mathrm{xa}})}{\nu + M - 2} K_{\mathrm{aa}}^{-1}$$

$$\hat{m}_{\mathrm{u}_j}(\tilde{\mathrm{y}}_j) = \beta \hat{K}_{\mathrm{u}_j} K_{\mathrm{aa}}^{-1} K_{\mathrm{xa}}^T \tilde{\mathrm{y}}_j, \tag{31}$$

and $\{/(\tilde{\mathrm{y}}_j, \mathrm{u}_j)\}$ represents all those terms which are independent of both $\tilde{\mathrm{y}}_j$ and u_j. The constant of proportionality in (29) is chosen to exclude $(\tilde{\mathrm{y}}_j, \mathrm{u}_j)-$independent terms in the expression for $\mu_{\mathrm{y}_j;\mathrm{u}_j}$, i.e.,

$$\mu_{\mathrm{y}_j;\mathrm{u}_j}(\tilde{\mathrm{y}}_j) = \exp\left((\mathrm{u}_j)^T \hat{K}_{\mathrm{u}_j}^{-1} \hat{m}_{\mathrm{u}_j}(\tilde{\mathrm{y}}_j) \right. \tag{32}$$

$$\left. -0.5(\mathrm{u}_j)^T \hat{K}_{\mathrm{u}_j}^{-1} \mathrm{u}_j + 0.5(\mathrm{u}_j)^T K_{\mathrm{aa}}^{-1} \mathrm{u}_j - 0.5\beta\|\tilde{\mathrm{y}}_j\|^2 \right).$$

Definition 8 (Data-Model): y_j is represented by means of a membership function, $\mu_{\mathrm{y}_j} : \mathbb{R}^N \to [0, 1]$, as

$$\mu_{\mathrm{y}_j}(\tilde{\mathrm{y}}_j) \propto \exp\left(\left\langle \log(\mu_{\mathrm{y}_j;\mathrm{u}_j}(\tilde{\mathrm{y}}_j)) \right\rangle_{\mu_{\mathrm{u}_j}} \right) \tag{33}$$

where $\mu_{\mathrm{y}_j;\mathrm{u}_j}$ is given by (32) and $\mu_{\mathrm{u}_j} : \mathbb{R}^M \to [0, 1]$ is a membership function representing u_j. Thus, μ_{y_j} is obtained from $\log(\mu_{\mathrm{y}_j;\mathrm{u}_j})$ after averaging out the auxiliary-outputs u_j using membership function μ_{u_j}.

C. Variational Optimization of Data-Model

The data model (33) involves the membership function μ_{u_j}. To determine μ_{u_j} for a given y_j, $\log(\mu_{\mathrm{y}_j}(\mathrm{y}_j))$ is maximized w.r.t. μ_{u_j} around an initial guess. The zero-mean Gaussian membership function with covariance as equal to K_{aa} is taken as the initial guess. It follows from (33) that maximization of $\log(\mu_{\mathrm{y}_j}(\mathrm{y}_j))$ is equivalent to the maximization of $\left\langle \log(\mu_{\mathrm{y}_j;\mathrm{u}_j}(\mathrm{y}_j)) \right\rangle_{\mu_{\mathrm{u}_j}}$.

Result 1: The solution of following maximization problem:

$$\mu_{\mathrm{u}_j}^* = \arg \max_{\mu_{\mathrm{u}_j}} \left[\left\langle \log(\mu_{\mathrm{y}_j;\mathrm{u}_j}(\mathrm{y}_j)) \right\rangle_{\mu_{\mathrm{u}_j}} \right. \tag{34}$$

$$\left. - \left\langle \log\left(\frac{\mu_{\mathrm{u}_j}(\mathrm{u}_j)}{\exp\left(-0.5(\mathrm{u}_j)^T K_{\mathrm{aa}}^{-1} \mathrm{u}_j \right)} \right) \right\rangle_{\mu_{\mathrm{u}_j}} \right]$$

under the fixed integral constraint:

$$\int_{\mathbb{R}^M} \mu_{\mathrm{u}_j} \ \mathrm{d}\lambda^M = C_{\mathrm{u}_j} > 0 \tag{35}$$

where the value of C_{u_j} is so chosen such that the maximum possible values of $\mu_{\mathrm{u}_j}^*$ remain as equal to unity, is given as

$$\mu_{\mathrm{u}_j}^*(\mathrm{u}_j) = \tag{36}$$

$$\exp\left(-0.5 \left(\mathrm{u}_j - \hat{m}_{\mathrm{u}_j}(\mathrm{y}_j) \right)^T \hat{K}_{\mathrm{u}_j}^{-1} \left(\mathrm{u}_j - \hat{m}_{\mathrm{u}_j}(\mathrm{y}_j) \right) \right)$$

where $\hat{K}_{\mathrm{u}_j}$ and $\hat{m}_{\mathrm{u}_j}$ are given by (30) and (31) respectively. The solution of the optimization problem results in

$$\mu_{\mathrm{y}_j}(\tilde{\mathrm{y}}_j) \propto \exp\left(\{/(\mathrm{y}_j, \tilde{\mathrm{y}}_j)\} \right. \tag{37}$$

$$- 0.5\beta \left\{ \|\tilde{\mathrm{y}}_j\|^2 - 2 \left(\hat{m}_{\mathrm{u}_j}(\mathrm{y}_j) \right)^T K_{\mathrm{aa}}^{-1} K_{\mathrm{xa}}^T \tilde{\mathrm{y}}_j \right.$$

$$+ \left(\hat{m}_{\mathrm{u}_j}(\mathrm{y}_j) \right)^T K_{\mathrm{aa}}^{-1} K_{\mathrm{xa}}^T K_{\mathrm{xa}} K_{\mathrm{aa}}^{-1} \hat{m}_{\mathrm{u}_j}(\mathrm{y}_j)$$

$$\left. \left. + \frac{\mathrm{tr}(K_{\mathrm{xx}} - K_{\mathrm{aa}}^{-1} K_{\mathrm{xa}}^T K_{\mathrm{xa}})}{\nu + M - 2} \left(\hat{m}_{\mathrm{u}_j}(\mathrm{y}_j) \right)^T K_{\mathrm{aa}}^{-1} \hat{m}_{\mathrm{u}_j}(\mathrm{y}_j) \right\} \right)$$

where $\{/(\mathrm{y}_j, \tilde{\mathrm{y}}_j)\}$ represents all $(\mathrm{y}_j, \tilde{\mathrm{y}}_j)-$independent terms.

Proof: The proof is similar to as that of Result 2 in [24]. ∎

The constant of proportionality in (37) is chosen to exclude $(\mathrm{y}_j, \tilde{\mathrm{y}}_j)-$independent terms resulting in

$$
\mu_{\mathrm{y}_j}(\tilde{\mathrm{y}}_j) = \exp\left(-\frac{\beta}{2}\left\{\|\tilde{\mathrm{y}}_j\|^2 - 2\left(\hat{m}_{\mathrm{u}_j}(\mathrm{y}_j)\right)^T K_{\mathrm{aa}}^{-1} K_{\mathrm{xa}}^T \tilde{\mathrm{y}}_j \right.\right. \quad (38)
$$
$$
+ \left(\hat{m}_{\mathrm{u}_j}(\mathrm{y}_j)\right)^T K_{\mathrm{aa}}^{-1} K_{\mathrm{xa}}^T K_{\mathrm{xa}} K_{\mathrm{aa}}^{-1} \hat{m}_{\mathrm{u}_j}(\mathrm{y}_j)
$$
$$
\left.\left. + \left(\hat{m}_{\mathrm{u}_j}(\mathrm{y}_j)\right)^T \frac{\mathrm{tr}(K_{\mathrm{xx}} - K_{\mathrm{aa}}^{-1} K_{\mathrm{xa}}^T K_{\mathrm{xa}})}{\nu + M - 2} K_{\mathrm{aa}}^{-1} \hat{m}_{\mathrm{u}_j}(\mathrm{y}_j)\right\}\right).
$$

D. Estimation of Membership-Mapping Parameters

Definition 9 (Averaged Estimation of Membership-Mapping Output): $\mathcal{F}_j(x^i)$ (which is the $i-$th element of vector f_j (20)) can be estimated as

$$
\widehat{\mathcal{F}_j(x^i)} := \left\langle \left\langle (\mathrm{f}_j)_i \right\rangle_{\mu_{\mathrm{f}_j;\mathrm{u}_j}} \right\rangle_{\mu_{\mathrm{u}_j}^*} \quad (39)
$$

where $(\mathrm{f}_j)_i$ denotes the $i-$th element of f_j, $\mu_{\mathrm{f}_j;\mathrm{u}_j}$ is defined as in (22), and $\mu_{\mathrm{u}_j}^*$ is the optimal membership function (36) representing u_j. That is, $\mathcal{F}_j(x^i)$, being a function of u_j, is averaged over u_j for an estimation.

Let $G(x) \in \mathbb{R}^{1 \times M}$ be a vector-valued function defined as

$$
G(x) := \begin{bmatrix} kr(x, a^1) & \cdots & kr(x, a^M) \end{bmatrix} \quad (40)
$$

where $kr : \mathbb{R}^n \times \mathbb{R}^n \to \mathbb{R}$ is defined as in (11). It is shown in Appendix A that

$$
\widehat{\mathcal{F}_j(x^i)} = G(x^i)\left(K_{\mathrm{xa}}^T K_{\mathrm{xa}} + \tau K_{\mathrm{aa}} + \beta^{-1} K_{\mathrm{aa}}\right)^{-1} K_{\mathrm{xa}}^T \mathrm{y}_j \quad (41)
$$

where τ is given as

$$
\tau := \frac{\mathrm{tr}(K_{\mathrm{xx}} - K_{\mathrm{aa}}^{-1} K_{\mathrm{xa}}^T K_{\mathrm{xa}})}{\nu + M - 2}. \quad (42)
$$

Define a vector $\alpha_j \in \mathbb{R}^M$ as

$$
\alpha_j(\beta^{-1}) := \left(K_{\mathrm{xa}}^T K_{\mathrm{xa}} + \tau K_{\mathrm{aa}} + \beta^{-1} K_{\mathrm{aa}}\right)^{-1} (K_{\mathrm{xa}})^T \mathrm{y}_j \quad (43)
$$

so that $\widehat{\mathcal{F}_j(x^i)}$ could be expressed as

$$
\widehat{\mathcal{F}_j(x^i)} = \left(G(x^i)\right) \alpha_j(\beta^{-1}). \quad (44)
$$

It follows from (44) that estimation of the membership-mapping outputs requires computing α_j via (43) which in-turn requires estimating the inverse precision value β^{-1}. The inverse precision value β^{-1} is iteratively estimated as the inverse of the mean squared error between data and membership-mappings outputs. That is,

$$
\beta^{-1} = \frac{1}{pN} \sum_{j=1}^{p} \sum_{i=1}^{N} \left|y_j^i - \widehat{\mathcal{F}_j(x^i)}\right|^2 \quad (45)
$$

where $\widehat{\mathcal{F}_j(x^i)}$ is the estimated membership-mapping output given as in (44). Expression (45) using (44) can be expressed as

$$
\beta^{-1} = \frac{1}{pN} \sum_{j=1}^{p} \sum_{i=1}^{N} \left|y_j^i - \left(G(x^i)\right) \alpha_j(\beta^{-1})\right|^2. \quad (46)
$$

As $G(x^i)$ is equal to the $i-$th row of matrix K_{xa}, (46) can be expressed as

$$
\beta^{-1} = \frac{1}{pN} \sum_{j=1}^{p} \|\mathrm{y}_j - K_{\mathrm{xa}} \alpha_j(\beta^{-1})\|^2. \quad (47)
$$

We suggest to estimate β^{-1} and α_j iteratively using (47) and (43) till the convergence.

IV. A GLOBALLY CONVERGENT LEARNING ALGORITHM AND ROBUSTNESS ANALYSIS FOR VARIATIONAL MEMBERSHIP-MAPPINGS

A. Convergence Analysis

In this subsection, we study the convergence of estimation algorithm (47, 43). In particular, we derive a sufficient condition for estimation algorithm (47, 43) to converge. For this, consider the singular value decomposition of K_{xa}:

$$
K_{\mathrm{xa}} = U \begin{bmatrix} S \\ 0 \end{bmatrix} V^T \quad (48)
$$

where $U \in \mathbb{R}^{N \times N}$ and $V \in \mathbb{R}^{M \times M}$ are orthogonal, and $S = \mathrm{diag}(s_1, \cdots, s_M)$ is a diagonal matrix with $s_1 \geq s_2 \geq \cdots \geq s_M \geq 0$ being the singular values of K_{xa}. The vectors $b_j^1 \in \mathbb{R}^M$ and $b_j^2 \in \mathbb{R}^{N-M}$ are defined as

$$
\begin{bmatrix} b_j^1 \\ b_j^2 \end{bmatrix} = U^T \mathrm{y}_j. \quad (49)
$$

The expression (43) for α_j can be rewritten as

$$
\alpha_j(\beta^{-1}) = \left(V S^2 V^T + \tau K_{\mathrm{aa}} + \beta^{-1} K_{\mathrm{aa}}\right)^{-1} V S b_j^1. \quad (50)
$$

Consider

$$
\mathrm{y}_j - K_{\mathrm{xa}} \alpha_j(\beta^{-1}) = U U^T \mathrm{y}_j \quad (51)
$$
$$
- U \begin{bmatrix} S \\ 0 \end{bmatrix} V^T \left(V S^2 V^T + (\tau + \beta^{-1}) K_{\mathrm{aa}}\right)^{-1} V S b_j^1.
$$

Using matrix inversion lemma,

$$
\mathrm{y}_j - K_{\mathrm{xa}} \alpha_j(\beta^{-1}) = \quad (52)
$$
$$
U \begin{bmatrix} \left(I + \frac{1}{\tau+\beta^{-1}} S V^T K_{\mathrm{aa}}^{-1} V S\right)^{-1} b_j^1 \\ b_j^2 \end{bmatrix},
$$

and hence,

$$
\|\mathrm{y}_j - K_{\mathrm{xa}} \alpha_j(\beta^{-1})\|^2 = \|b_j^2\|^2 \quad (53)
$$
$$
+ (\tau + \beta^{-1})^2 (b_j^1)^T \left((\tau + \beta^{-1})I + S V^T K_{\mathrm{aa}}^{-1} V S\right)^{-2} b_j^1
$$

Using (53) in (47),

$$
\beta^{-1} = \frac{1}{pN} \sum_{j=1}^{p} \|b_j^2\|^2 \quad (54)
$$
$$
+ \frac{(\tau + \beta^{-1})^2}{pN} \sum_{j=1}^{p} (b_j^1)^T \left((\tau + \beta^{-1})I + S V^T K_{\mathrm{aa}}^{-1} V S\right)^{-2} b_j^1.
$$

Result 2 (A Function in β^{-1}): Let $\mathcal{R}$ be a function in β^{-1} defined as

$$\mathcal{R}(\beta^{-1}) := \frac{1}{pN} \sum_{j=1}^{p} \|b_j^2\|^2 \tag{55}$$

$$+ \frac{(\tau + \beta^{-1})^2}{pN} \sum_{j=1}^{p} (b_j^1)^T \left((\tau + \beta^{-1})I + SV^T K_{aa}^{-1} VS \right)^{-2} b_j^1.$$

We have followings:

1) $\mathcal{R}(\beta^{-1}) \in \left(\beta^{-1}|_{low}, \beta^{-1}|_{up}\right), \forall \beta^{-1} \in \mathbb{R}_{>0}$, where

$$\beta^{-1}|_{low} = \frac{1}{pN} \sum_{j=1}^{p} \|b_j^2\|^2 \tag{56}$$

$$\beta^{-1}|_{up} = \frac{1}{pN} \sum_{j=1}^{p} \|y_j\|^2. \tag{57}$$

2) The lower and upper bounds on the derivative of $\mathcal{R}$ w.r.t. β^{-1} are given as

$$0 < \frac{d\mathcal{R}(\beta^{-1})}{d\beta^{-1}} < \frac{2}{pN} \frac{1}{\tau + \beta^{-1}} \sum_{j=1}^{p} \|b_j^1\|^2. \tag{58}$$

3) $\mathcal{R}(\beta^{-1})$ has at least one fixed point in $\left(\beta^{-1}|_{low}, \beta^{-1}|_{up}\right)$.

Proof: The proof is provided in Appendix B. ∎

Result 3 (Convergence): If τ is chosen such that

$$\tau > \frac{2}{pN} \sum_{j=1}^{p} \|y_j\|^2 - \frac{1}{pN} \sum_{j=1}^{p} \|b_j^2\|^2, \tag{59}$$

then the iterations

$$\beta^{-1}|_{it+1} = \mathcal{R}(\beta^{-1}|_{it}), \ it \in \{0,1,2,\cdots\}, \tag{60}$$

with $\beta^{-1}|_0 \in \left(\beta^{-1}|_{low}, \beta^{-1}|_{up}\right)$, converge to the unique fixed point of $\mathcal{R}(\beta^{-1})$.

Proof: The proof is provided in Appendix C. ∎

B. Learning Algorithm

Result 3 allows to design a globally convergent algorithm for the variational learning of membership-mappings via ensuring the sufficient condition (59). For this, it is observed that τ, defined as in (42), is a function of parameters set $\{M, \sigma^2, \{w_i\}_{i=1}^{n}, x, a, \nu\}$. It follows from the kernel function definition (11) that

$$\tau(M, \sigma^2, \{w_i\}_{i=1}^{n}, x, a, \nu) = \sigma^2 \tau(M, 1, \{w_i\}_{i=1}^{n}, x, a, \nu). \tag{61}$$

Using (61), the condition (59) can be rewritten as

$$\sigma^2 > \frac{1}{\tau(M, 1, \{w_i\}_{i=1}^{n}, x, a, \nu)} \frac{\sum_{j=1}^{p}(2\|y_j\|^2 - \|b_j^2\|^2)}{pN}. \tag{62}$$

To hold the inequality (62), the value of σ^2 is adjusted as in the following:

if $\tau(M, 1, \{w_i\}_{i=1}^{n}, x, a, \nu) > \frac{\sum_{j=1}^{p}(2\|y_j\|^2 - \|b_j^2\|^2)}{pN}$ **then**
  $\sigma^2 = 1$
else
  $\sigma^2 = \frac{1.1}{\tau(M,1,\{w_i\}_{i=1}^{n},x,a,\nu)} \frac{\sum_{j=1}^{p}(2\|y_j\|^2 - \|b_j^2\|^2)}{pN}.$
end if

Further, some of the parameters must be prior chosen which are suggested to be chosen as in the following:

a) Auxiliary inducing points: The auxiliary inducing points are suggested to be chosen as the cluster centroids:

$$a = \{a^m\}_{m=1}^{M} = cluster\_centroid(\{x^i\}_{i=1}^{N}, M) \tag{63}$$

where $cluster\_centroid(\{x^i\}_{i=1}^{N}, M)$ represents the k-means clustering on $\{x^i\}_{i=1}^{N}$.

b) Degrees of freedom: The degrees of freedom associated to the Student-t membership-mapping $\nu \in \mathbb{R}_+ \setminus [0,2]$ is chosen as

$$\nu = 2.1 \tag{64}$$

c) Parameters $(w_1, \cdots, w_n)$: The parameters $(w_1, \cdots, w_n)$ for kernel function (11) are chosen such that w_k (for $k \in \{1, 2, \cdots, n\}$) is given as

$$w_k = \left(\max_{1 \le i \le N} (x_k^i) - \min_{1 \le i \le N} (x_k^i) \right)^{-2} \tag{65}$$

where x_k^i is the $k-$th element of vector $x^i \in \mathbb{R}^n$.

Finally, Algorithm 1 presents a systematic procedure for the variational learning of membership-mappings while ensuring the sufficient condition (59) for the convergence.

Algorithm 1 A globally convergent algorithm for the variational learning of membership-mappings

---

Require: Dataset $\{(x^i, y^i) \mid i \in \{1, \cdots, N\}\}$ and maximum possible number of auxiliary points $M_{max} \in \mathbb{Z}_+$ with $M_{max} \le N$.
1: Choose ν and $w = (w_1, \cdots, w_n)$ as in (64) and (65) respectively.
2: Set iteration count $it = 0$, $M|_0 = M_{max}$, and determine $a|_0 = \{a^m|_0\}_{m=1}^{M|_0}$ using (63).
3: **while** $\tau(M|_{it}, 1, \{w_i\}_{i=1}^{n}, x, a|_{it}, \nu) \le 0$ **do**
4:   $M|_{it+1} = M|_{it} - 1$
5:   Determine $a|_{it+1} = \{a^m|_{it+1}\}_{m=1}^{M|_{it+1}}$ using (63).
6:   $it \leftarrow it + 1$
7: **end while**
8: Set $M = M|_{it}$ and compute $a = \{a^m\}_{m=1}^{M}$ using (63).
9: Compute K_{xa} using (26) taking $\sigma^2 = 1$ and perform singular value decomposition of K_{xa} to compute orthogonal matrix U such that (48) holds. Further compute b_j^1 and b_j^2 using (49) for all $j \in \{1, \cdots, p\}$.
10: **if** $\tau(M, 1, \{w_i\}_{i=1}^{n}, x, a, \nu) > \frac{\sum_{j=1}^{p}(2\|y_j\|^2 - \|b_j^2\|^2)}{pN}$ **then**
11:   $\sigma^2 = 1$
12: **else**
13:   $\sigma^2 = \frac{1.1}{\tau(M,1,\{w_i\}_{i=1}^{n},x,a,\nu)} \frac{\sum_{j=1}^{p}(2\|y_j\|^2 - \|b_j^2\|^2)}{pN}.$
14: **end if**
15: Compute $a = \{a^m\}_{m=1}^{M}$ using (63), K_{xx} using (10), K_{aa} using (25), and K_{xa} using (26).
16: Compute τ using (42).
17: Set iteration count $it = 0$ and $\beta^{-1}|_0 = 0.5(\beta^{-1}|_{low} + \beta^{-1}|_{up})$, where $\beta^{-1}|_{low}$ and $\beta^{-1}|_{up}$ are given by (56) and (57) respectively.
18: Determine the unique fixed point of $\mathcal{R}(\beta^{-1})$, say $\hat{\beta}^{-1}$, using iterations (60).
19: Compute matrix $\alpha = \begin{bmatrix} \alpha_1(\hat{\beta}^{-1}) & \cdots & \alpha_p(\hat{\beta}^{-1}) \end{bmatrix} \in \mathbb{R}^{M \times p}$, where $\alpha_j(\hat{\beta}^{-1})$, $j \in \{1, \cdots, p\}$, is computed using (43).
20: **return** the parameters set $\mathbb{M} = \{\alpha, a, M, \sigma, w, \hat{\beta}\}$.

Definition 10 (Membership-Mappings Prediction): Given the parameters set $\mathbb{M} = \{\alpha, a, M, \sigma, w, \hat{\beta}\}$ returned by Algorithm 1, the learned membership-mappings could be used to predict output corresponding to any arbitrary input data point $x \in \mathbb{R}^n$ as

$$\hat{y}(x; \mathbb{M}) = \begin{bmatrix} \widehat{\mathcal{F}_1(x)} & \cdots & \widehat{\mathcal{F}_p(x)} \end{bmatrix}^T \tag{66}$$

where $\widehat{\mathcal{F}_j(x)}$, defined as in (44), is the estimated output of $j-$th membership-mapping. It follows from (44) that

$$\hat{y}(x; \mathbb{M}) = (\alpha(\hat{\beta}))^T (G(x))^T \tag{67}$$

where $G(\cdot) \in \mathbb{R}^{1 \times M}$ is a vector-valued function (40).

As a CDMMA consists of membership-mapping compositions, Algorithm 1 can be directly applied for their learning as in Algorithm 2 and Algorithm 3. For practical applications, Algorithm 3 is suggested for the learning of wide CDMMA where a computational optimization of a free parameter is performed via minimizing the estimated variance of the mean squared error between data and membership-mappings outputs.

Algorithm 2 A globally convergent algorithm for the variational learning of CDMMA

Require: Data set $\mathbf{Y} = \{y^i \in \mathbb{R}^p \mid i \in \{1, \cdots, N\}\}$; the subspace dimension $n \in \{1, 2, \cdots, p\}$; maximum number of auxiliary points $M_{max} \in \mathbb{Z}_+$ with $M_{max} \leq N$; the number of layers $L \in \mathbb{Z}_+$.

1: **for** $l = 1$ to L **do**
2:      Set subspace dimension associated to $l-$th layer as $n_l = \max(n - l + 1, 1)$.
3:      Define $P^l \in \mathbb{R}^{n_l \times p}$ such that $i-$th row of P^l is equal to transpose of eigenvector corresponding to $i-$th largest eigenvalue of sample covariance matrix of data set $\mathbf{Y}$.
4:      Define a latent variable $x^{l,i} \in \mathbb{R}^{n_l}$, for $i \in \{1, \cdots, N\}$, as

$$x^{l,i} := \begin{cases} P^l y^i & \text{if } l = 1, \\ P^l \hat{y}^{l-1}(x^{l-1,i}; \mathbb{M}^{l-1}) & \text{if } l > 1 \end{cases} \tag{68}$$

     where $\hat{y}^{l-1}$ is the estimated output of the $(l-1)-$th layer computed using (67) for the parameters set $\mathbb{M}^{l-1} = \{\alpha^{l-1}, \mathrm{a}^{l-1}, M^{l-1}, \sigma^{l-1}, w^{l-1}\}$.
5:      Define M_{max}^l as

$$M_{max}^l := \begin{cases} M_{max} & \text{if } l = 1 \\ M^{l-1} & \text{if } l > 1 \end{cases} \tag{69}$$

6:      Compute parameters set $\mathbb{M}^l = \{\alpha^l, \mathrm{a}^l, M^l, \sigma^l, w^l, \hat{\beta}^l\}$, characterizing the membership-mappings associated to $l-$th layer, using Algorithm 1 on data set $\{(x^{l,i}, y^i) \mid i \in \{1, \cdots, N\}\}$ with maximum possible number of auxiliary points M_{max}^l.
7: **end for**
8: **return** the parameters set $\mathcal{M} = \{\{\mathbb{M}^1, \cdots, \mathbb{M}^L\}, \{P^1, \cdots, P^L\}\}$.

Definition 11 (CDMMA Filtering): Given a CDMMA with its parameters being represented by a set $\mathcal{M} = \{\{\mathbb{M}^1, \cdots, \mathbb{M}^L\}, \{P^1, \cdots, P^L\}\}$, the autoencoder can be applied for filtering a given input vector $y \in \mathbb{R}^p$ as follows:

$$x^l(y; \mathcal{M}) = \begin{cases} P^l y, & l = 1 \\ P^l \hat{y}^{l-1}(x^{l-1}; \mathbb{M}^{l-1}) & l \geq 2 \end{cases} \tag{70}$$

Here, $\hat{y}^{l-1}$ is the output of the $(l-1)-$th layer estimated using (67). Finally, CDMMA's output, $\mathcal{D}(y; \mathcal{M})$, is given as

$$\widehat{\mathcal{D}}(y; \mathcal{M}) = \hat{y}^{l^*}(x^{l^*}; \mathbb{M}^{l^*}) \tag{71}$$

$$l^* = \arg \min_{l \in \{1, \cdots, L\}} \|y - \hat{y}^l(x^l; \mathbb{M}^l)\|^2. \tag{72}$$

Definition 12 (Wide CDMMA Filtering): Given a wide CDMMA with its parameters being represented by a set $\mathcal{P} = \{\mathcal{M}^s\}_{s=1}^S$, the autoencoder can be applied for filtering a given input vector $y \in \mathbb{R}^p$ as follows:

$$\widehat{\mathcal{WD}}(y; \mathcal{P}) = \widehat{\mathcal{D}}(y; \mathcal{M}^{s^*}) \tag{73}$$

$$s^* = \arg \min_{s \in \{1, 2, \cdots, S\}} \|y - \widehat{\mathcal{D}}(y; \mathcal{M}^s)\|^2, \tag{74}$$

Algorithm 3 A globally convergent algorithm for the variational learning of wide CDMMA

Require: Data set $\mathbf{Y} = \{y^i \in \mathbb{R}^p \mid i \in \{1, \cdots, N\}\}$; the number of layers $L \in \mathbb{Z}_+$; the subspace dimension $n \in \{1, 2, \cdots, p\}$; an array of possible r_{max} values $\{r_{max}^1, \cdots, r_{max}^{N_r}\}$ with $0 < r_{max}^1 < r_{max}^2 < \cdots < r_{max}^{N_r} \leq 1$.

1: Apply k-means clustering to partition $\mathbf{Y}$ into S subsets, $\{\mathbf{Y}^1, \cdots, \mathbf{Y}^S\}$, where $S = \lceil N/1000 \rceil$.
2: **for** $s = 1$ to S **do**
3:      **for** $r = r_{max}^1$ to $r = r_{max}^{N_r}$ **do**
4:          Apply Algorithm 2 on $\mathbf{Y}^s$ to build a single-layered CDMMA, $\mathcal{M}^r = \{\{\mathbb{M}^{1,r}\}, \{P^{1,r}\}\}$ where $\mathbb{M}^{1,r} = \{\alpha^{1,r}, \mathrm{a}^{1,r}, M^{1,r}, \sigma^{1,r}, w^{1,r}, \hat{\beta}^{1,r}\}$, taking n as the subspace dimension; maximum number of auxiliary points as equal to $r \times \#\mathbf{Y}^s$ (where $\#\mathbf{Y}^s$ is the number of data points in $\mathbf{Y}^s$); and $L = 1$.
5:      **end for**
6:      Set $r_{max} = \arg \max_{r \in \{r_{max}^1, r_{max}^2, \cdots, r_{max}^{N_r}\}} \hat{\beta}^{1,r}$.
7:      Build a CDMMA, $\mathcal{M}^s$, by applying Algorithm 2 on $\mathbf{Y}^s$ taking n as the subspace dimension; maximum number of auxiliary points as equal to $r_{max} \times \#\mathbf{Y}^s$ (where $\#\mathbf{Y}^s$ is the number of data points in $\mathbf{Y}^s$); and L as the number of layers.
8: **end for**
9: **return** the parameters set $\mathcal{P} = \{\mathcal{M}^s\}_{s=1}^S$.

---

where $\widehat{\mathcal{D}}(y; \mathcal{M}^s)$ is the output of $s-$th CDMMA estimated using (71).

C. Robustness Analysis

Consider that the data samples $\{(x^i, y^i) \mid i \in \{1, \cdots, N\}\}$ are subject to deterministic perturbations and thus matrix K_{xa} (26) and vector y_j (19) are subject to perturbations. Let $\Delta K_{\mathrm{xa}} \in \mathbb{R}^{N \times M}$ and $\Delta \mathrm{y}_j \in \mathbb{R}^N$ be the unknown (but bounded) perturbations in K_{xa} and y_j respectively due to the perturbations in the data samples. The data model assumes that there exists some parameters vector $\alpha_j^* \in \mathbb{R}^M$ such that

$$\mathrm{y}_j + \Delta \mathrm{y}_j = (K_{\mathrm{xa}} + \Delta K_{\mathrm{xa}})\alpha_j^*. \tag{75}$$

The modeling problem is concerned with the estimation of α_j^* in the presence of unknown perturbations ΔK_{xa} and $\Delta \mathrm{y}_j$. To show that Algorithm 1 provides a robust estimation of α_j^*, define

$$\Delta_x := \Delta K_{\mathrm{xa}}(K_{\mathrm{aa}}^{1/2})^{-1} \tag{76}$$

where $K_{\mathrm{aa}}^{1/2}$ is the unique square root of positive definite matrix K_{aa} (25). The set of equations (75) can be expressed as

$$\mathrm{y}_j + \Delta \mathrm{y}_j = (K_{\mathrm{xa}} + \Delta_x K_{\mathrm{aa}}^{1/2})\alpha_j^*. \tag{77}$$

The perturbation matrix $[\Delta_x \ \Delta \mathrm{y}_j]$ is unknown, however, is assumed bounded. That is, there exists a scalar $\delta_m > 0$ such that $\|[\Delta_x \ \Delta \mathrm{y}_j]\|_F \leq \delta_m$, where $\|\cdot\|_F$ denotes the Frobenius norm. A robust solution to the estimation of parameters seeks to alleviate the worst-case effect of perturbations. For example, the worst-case residual error can be minimized via solving a min-max estimation problem as in Result 4.
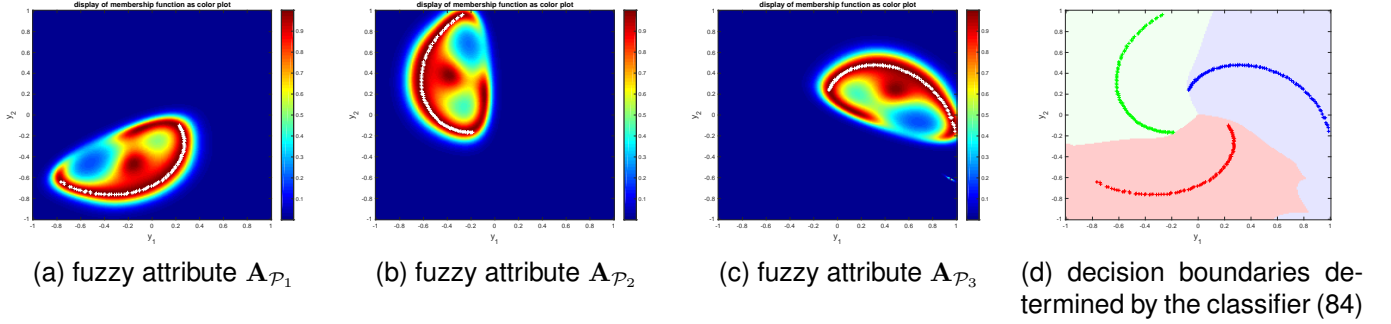
Fig. 1. A few examples of fuzzy attributes induced by deep autoencoders. The given set of 100 two-dimensional data samples, marked as '+' in the figures, has been used to train a wide conditionally deep membership-mapping autoencoder using Algorithm 3 taking $L = 5$, $n = 2$, and possible r_{max} values as $\{0.01, 0.02, \cdots, 0.1\}$. The membership function associated to a fuzzy attribute has been defined by (81) taking $\nu = 2.001$.

Result 4 (Robustness): Algorithm 1 provides a robust estimation of α_j^* via solving the following min-max estimation problem:

$$\hat{\alpha}_j = \arg \min_{\alpha_j^*} \tag{78}$$

$$\max_{\|[\Delta_x \ \Delta \mathbf{y}_j]\|_F \leq \delta_m} \left\| (K_{\mathrm{xa}} + \Delta_x K_{\mathrm{aa}}^{1/2})\alpha_j^* - (\mathbf{y}_j + \Delta \mathbf{y}_j) \right\|,$$

where the upper-bound on the norm of perturbation matrix is given as

$$\delta_m = \tag{79}$$

$$\frac{\sqrt{1 + \|K_{\mathrm{aa}}^{1/2}(K_{\mathrm{xa}}^T K_{\mathrm{xa}} + \tau K_{\mathrm{aa}} + \hat{\beta}^{-1}K_{\mathrm{aa}})^{-1}K_{\mathrm{xa}}^T \mathbf{y}_j\|^2}}{\|((\tau + \hat{\beta}^{-1})I + K_{\mathrm{xa}}K_{\mathrm{aa}}^{-1}K_{\mathrm{xa}}^T)^{-1}\mathbf{y}_j\|},$$

where $\hat{\beta}^{-1}$ is the unique fixed point of $\mathcal{R}(\beta^{-1})$ to which the iterations (60) converge.

Proof: The proof is provided in Appendix D. ∎

V. SECURE DISTRIBUTED DEEP LEARNING

A. Fuzzy Attributes and Classification Applications

Definition 13 (A Fuzzy Attribute Induced by Deep Membership-Mapping Autoencoder): A fuzzy attribute $\mathbf{A}_{\mathcal{P}}$, associated to a wide conditionally deep membership-mapping autoencoder $\mathcal{P}$ (that has been learned using dataset $\mathbf{Y} \subset \mathbb{R}^p$), can be defined on a universe of discourse $\mathbb{R}^p$ as

$$\mathbf{A}_{\mathcal{P}} := \{(y, \mu_{\mathbf{A}_{\mathcal{P}}}(y)) \mid y \in \mathbb{R}^p\} \tag{80}$$

where $\mu_{\mathbf{A}_{\mathcal{P}}}(y) : \mathbb{R}^p \to [0,1]$ is a $p-$variate membership function such that $\mu_{\mathbf{A}_{\mathcal{P}}}(y)$ is interpreted as the degree to which a point $y \in \mathbb{R}^p$ matches to the attribute $\mathbf{A}_{\mathcal{P}}$. Without the loss of generality, the following Student-t type membership function can be defined to characterize $\mathbf{A}_{\mathcal{P}}$:

$$\mu_{\mathbf{A}_{\mathcal{P}}}(y) = \left(1 + \frac{1}{\nu - 2}\|y - \widehat{\mathcal{WD}}(y; \mathcal{P})\|^2\right)^{-\frac{\nu + p}{2}}, \tag{81}$$

where $\widehat{\mathcal{WD}}(y; \mathcal{P})$ is through autoencoder $\mathcal{P}$ filtered output (73). Similarly, one can define Gaussian type of membership function:

$$\mu_{\mathbf{A}_{\mathcal{P}}}(y) = \exp\left(-\frac{1}{2p}\|y - \widehat{\mathcal{WD}}(y; \mathcal{P})\|^2\right). \tag{82}$$

A wide conditionally deep membership-mapping autoencoder induces a fuzzy attribute as defined in Definition 13. Fig. 1 provides three different examples of fuzzy attributes induced by the deep autoencoders. As demonstrated through color-plots in Fig. 1, the defined fuzzy attribute (Definition 13) learns a representation of the data samples. This motivates to define a fuzzy classifier based on the following if-then rules:

$$\text{If } y \text{ is } \mathbf{A}_{\mathcal{P}_1}, \text{ then the class is 1;}$$
$$\vdots \tag{83}$$
$$\text{If } y \text{ is } \mathbf{A}_{\mathcal{P}_C}, \text{ then the class is C.}$$

The class-label associated to a data point y is predicted based on fuzzy rules (83) as

$$\mathcal{C}(y; \{\mathcal{P}_c\}_{c=1}^C) = \arg \max_{1 \leq c \leq C} \mu_{\mathbf{A}_{\mathcal{P}_c}}(y). \tag{84}$$

The classifier (84), $\mathcal{C} : \mathbb{R}^p \to \{1, 2, \cdots, C\}$, assigns to an input vector the label of the class to which the data point has highest degree of matching. An example of the decision boundary determined by a three-class classifier is provided in Fig. 1.

B. Distributed Learning

We consider a scenario that data are distributed amongst different parties. Assume that there are K different datasets, $\{\mathbf{Y}^1, \cdots, \mathbf{Y}^K\}$, owned locally by K different parties. We consider the multi-class classification problem assuming that each local dataset, say $\mathbf{Y}^k$, can be partitioned into C different classes, i.e.,

$$\mathbf{Y}^k = \{\mathbf{Y}_1^k, \cdots, \mathbf{Y}_C^k\} \tag{85}$$

where $\mathbf{Y}_c^k$ refers to the $c-$th class labelled data samples owned locally by the $k-$th party. Let $\mathcal{P}_c^k$ be the wide conditionally deep membership-mapping autoencoder learned from $\mathbf{Y}_c^k$ and $\mathbf{A}_{\mathcal{P}_c^k}$ be the corresponding fuzzy attribute. The fuzzy classifier (83) can be extended for distributed setting as follows:

$$\text{If } y \text{ is } \mathbf{A}_{\mathcal{P}_1^1} \text{ OR } \mathbf{A}_{\mathcal{P}_1^2} \text{ OR } \cdots \text{ OR } \mathbf{A}_{\mathcal{P}_1^K}, \text{ then the class is 1;}$$
$$\vdots \tag{86}$$
$$\text{If } y \text{ is } \mathbf{A}_{\mathcal{P}_C^1} \text{ OR } \mathbf{A}_{\mathcal{P}_C^2} \text{ OR } \cdots \text{ OR } \mathbf{A}_{\mathcal{P}_C^K}, \text{ then the class is C.}$$
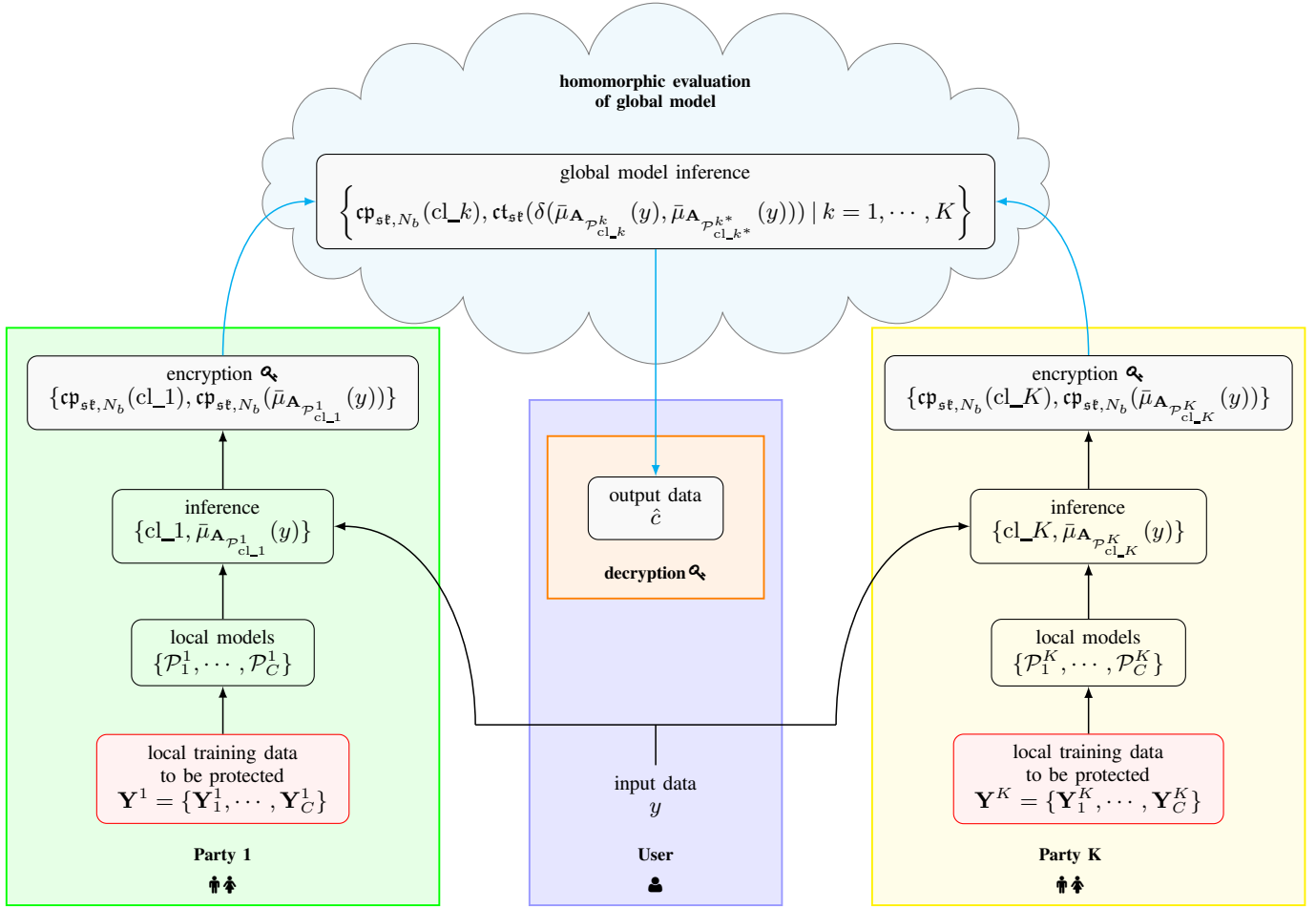
Fig. 2. A practical method for secure distributed deep learning based on membership-mappings and fully homomorphic encryption.

The class-label associated to a data point y is predicted based on fuzzy rules (86) as

$$\hat{c} = \arg \max_{1 \leq c \leq C} \left(\max_{1 \leq k \leq K} \mu_{\mathbf{A}_{\mathcal{P}_c^k}}(y) \right) \qquad (87)$$

$$= \arg \min_{1 \leq c \leq C} \left(\min_{1 \leq k \leq K} \left(1 - \mu_{\mathbf{A}_{\mathcal{P}_c^k}}(y) \right) \right) \qquad (88)$$

$$= \arg \min_{1 \leq c \leq C} \left(\min_{1 \leq k \leq K} \bar{\mu}_{\mathbf{A}_{\mathcal{P}_c^k}}(y) \right), \qquad (89)$$

where $\bar{\mu}_{\mathbf{A}_{\mathcal{P}_c^k}}(y) = 1 - \mu_{\mathbf{A}_{\mathcal{P}_c^k}}(y)$.

C. Secure Homomorphic Evaluation of Global Classifier

For a secure distributed learning based on fully homomorphic encryption, a practical approach is suggested based on the observation that instead of encrypting higher-dimensional vectors, it is sufficient to encrypt the scalar values $\{\bar{\mu}_{\mathbf{A}_{\mathcal{P}_c^k}}(y) \mid c = 1, \cdots, C; \ k = 1, \cdots, K\}$ for the homomorphic evaluation of classifier (86) (i.e. evaluation of (89)) in an efficient manner. That is, the homomorphic evaluation of the "arg min" function over $K \times C$ encrypted values is required. More efficiently, the homomorphic evaluation of the "arg min" function over K encrypted values is sufficient for the homomorphic evalu-

ation of the classifier. For this, define cl_k as the class-label predicted by the $k-$th local classifier, i.e.,

$$\mathrm{cl}\_k = \mathcal{C}(y; \{\mathcal{P}_c^k\}_{c=1}^C) \qquad (90)$$

where $\mathcal{C}(\cdot)$ is defined as in (84). Now, (89) can be alternatively expressed as

$$\hat{c} = \mathrm{cl}\_k^* \qquad (91)$$

$$k^* = \arg \min_{1 \leq k \leq K} \bar{\mu}_{\mathbf{A}_{\mathcal{P}_{\mathrm{cl}\_k}^k}}(y). \qquad (92)$$

Let $\delta(\mathfrak{m}_1, \mathfrak{m}_2)$ be the Kronecker delta function of two variables $\mathfrak{m}_1, \mathfrak{m}_2 \in [0,1]$ defined as

$$\delta(\mathfrak{m}_1, \mathfrak{m}_2) = \begin{cases} 1 & \text{if } \mathfrak{m}_1 = \mathfrak{m}_2, \\ 0 & \text{if } \mathfrak{m}_1 \neq \mathfrak{m}_2. \end{cases} \qquad (93)$$

It follows from (91-92) that

$$\hat{c} = \sum_{k=1}^{K} \mathrm{cl}\_k \ \delta \left(\bar{\mu}_{\mathbf{A}_{\mathcal{P}_{\mathrm{cl}\_k}^k}}(y), \bar{\mu}_{\mathbf{A}_{\mathcal{P}_{\mathrm{cl}\_k^*}^{k^*}}}(y) \right). \qquad (94)$$

A practical method using TFHE scheme [13], [14] is provided for secure distributed deep learning. For this, define the followings:

- For a given positive integer $N_b \in \mathbb{Z}_{>0}$, let $\mathfrak{pt}_{N_b} : [0,1] \to \{0,1,\cdots,2^{N_b}-1\}$ be a function defined as

$$\mathfrak{pt}_{N_b}(\mathfrak{m}) := \lceil (2^{N_b}-1)\mathfrak{m} \rceil, \ \mathfrak{m} \in [0,1]. \quad (95)$$

  In our setting, $\mathfrak{pt}_{N_b}(\mathfrak{m})$ is the plaintext that encodes a message $\mathfrak{m} \in [0,1]$ as unsigned N_b-bit integer.

- Let $\mathrm{BitDec}_{N_b} : \{0,1,\cdots,2^{N_b}-1\} \to \{0,1\}^{N_b}$ be the binary representation of a N_b-bit unsigned integer. That is,

$$(\mathfrak{bt}_1(\mathfrak{m}),\cdots,\mathfrak{bt}_{N_b}(\mathfrak{m})) = \mathrm{BitDec}_{N_b}(\mathfrak{pt}_{N_b}(\mathfrak{m})), \quad (96)$$

  where $\mathfrak{bt}_k(\mathfrak{m}) \in \{0,1\}$ for all $k \in \{1,2,\cdots,N_b\}$.

- Let N_c be the ciphertext dimension set for a given value of security bits, say 128 bits security.

- Let $\mathfrak{st} \in \{0,1\}^{N_c}$ be a secret key generated for TFHE encryption.

- Let $\mathfrak{ct}_{\mathfrak{st}}(\mathfrak{bt}) \in \mathbb{T}^{N_c+1}$, where $\mathbb{T} = \mathbb{R}/\mathbb{Z}$, be the TFHE encryption of a bit $\mathfrak{bt} \in \{0,1\}$, i.e., $\mathfrak{ct}_{\mathfrak{st}}(\mathfrak{bt}) = \mathrm{TFHE.Enc}(\mathfrak{bt};\mathfrak{st})$.

- Let $\mathfrak{cp}_{\mathfrak{st},N_b} : [0,1] \to \mathbb{T}^{N_b(N_c+1)}$ be a function defined as

$$\mathfrak{cp}_{\mathfrak{st},N_b}(\mathfrak{m}) := (\mathfrak{ct}_{\mathfrak{st}}(\mathfrak{bt}_1(\mathfrak{m})),\cdots,\mathfrak{ct}_{\mathfrak{st}}(\mathfrak{bt}_{N_b}(\mathfrak{m}))) \quad (97)$$

  where $\mathfrak{ct}_{\mathfrak{st}}(\mathfrak{bt}_k(\mathfrak{m}))$ is the TFHE encryption of bit $\mathfrak{bt}_k(\mathfrak{m})$. Thus, $\mathfrak{cp}_{\mathfrak{st},N_b}(\mathfrak{m})$ homomorphically encrypts the message $\mathfrak{m} \in [0,1]$ with N_b-bit precision.

Our approach to homomorphically evaluate the global classifier (86) is shown in Fig. 2. The approach consists of following steps:

1) A pair of secret and cloud keys is generated. The secret key is meant for encryption and decryption. The cloud key is exported to the cloud, and allows to operate over encrypted data.

2) For a given input y, the outputs of local classifiers $\{\mathfrak{cp}_{\mathfrak{st},N_b}(\mathrm{cl}\_k), \mathfrak{cp}_{\mathfrak{st},N_b}(\bar{\mu}_{\mathbf{A}_{\mathcal{P}^k_{\mathrm{cl}\_k}}}(y)) \mid k = 1,\cdots,K\}$ are sent to the cloud for performing secure homomorphic computations.

3) The values $\{\delta(\bar{\mu}_{\mathbf{A}_{\mathcal{P}^k_{\mathrm{cl}\_k}}}(y), \bar{\mu}_{\mathbf{A}_{\mathcal{P}^{k*}_{\mathrm{cl}\_k*}}}(y)) \mid k = 1,\cdots,K\}$ are homomorphically evaluated in the cloud from the encrypted data (sent by different parties) using a boolean circuit composed of bootstrapped binary gates.

4) The encrypted output of the global model $\{\mathfrak{cp}_{\mathfrak{st},N_b}(\mathrm{cl}\_k), \mathfrak{ct}_{\mathfrak{st}}(\delta(\bar{\mu}_{\mathbf{A}_{\mathcal{P}^k_{\mathrm{cl}\_k}}}(y), \bar{\mu}_{\mathbf{A}_{\mathcal{P}^{k*}_{\mathrm{cl}\_k*}}}(y))) \mid k = 1,\cdots,K\}$ is sent to the user.

5) The class-label associated to a data point y is predicted using (94) after decrypting the data provided by the cloud.

VI. EXPERIMENTS

The proposed method was implemented using MATLAB R2017b and TFHE C/C++ library [15] on a MacBook Pro machine with a 2.2 GHz Intel Core i7 processor and 16 GB of memory. The previous works [24], [26], [28] have already verified the competitive performance of membership-mappings in classification applications. In this study, our focus is to verify the application potential of the proposed approach and to compare the method with the alternative differentially private distributed deep learning approach [29], [30].

TABLE I
EXPERIMENTAL RESULTS ON MNIST DATASET

Method	Accuracy	Time
Proposed (8-bits precision of homomorphic computations)	0.9762	3.2251 s
Proposed (16-bits precision of homomorphic computations)	0.9872	4.9785 s
differentially private distributed deep learning with privacy-loss bound $\epsilon = 0.1$ [29]	0.0892	n/a
differentially private distributed deep learning with privacy-loss bound $\epsilon = 1$ [29]	0.8994	n/a

A. Details

Under a distributed deep learning scenario, the local models are developed using Algorithm 3 taking $L = 5$, $n = 20$, and possible r_{max} values array as $\{0.5\}$. Targeting 128-bits of security, TFHE library is used to homomorphically evaluate the global classifier with the precision of 16-bits and also 8-bits. For a comparison, differentially private local models, developed using Algorithm 3 on the noisy training data obtained via optimal noise adding mechanism [29], [30] (taking adjacency parameter $d = 1$, failure probability $\delta = 1\mathrm{e}-5$, and privacy-loss bound $\epsilon = 0.1$ and also $\epsilon = 1$), are combined through fuzzy rules (86) without any encryption. The test data accuracy and average computational time required for secure homomorphic computations in the cloud (for computing the encrypted global output for a given input) are considered as performance indices.

B. MNIST Dataset

The first experiment is on the widely used MNIST digits dataset containing 28×28 sized images divided into training set of 60000 images and testing set of 10000 images. The images' pixel values were divided by 255 to normalize the values in the range from 0 to 1. The 28×28 normalized values of each image were flattened to an equivalent $784-$dimensional data vector. A two-party scenario is considered such that Party-A owns all the training images of odd digits while Party-B owns the rest training images of even digits. Table I reports the experimental results.

C. Freiburg Groceries Dataset

The second experiment is on "Freiburg Groceries Dataset" considered previously [29] for privacy-preserving distributed learning experiments. The dataset contains 4947 labeled images of grocery products categorized into 25 different classes. A feature vector is created from each image by extracting features from "AlexNet" and "VGG-16" networks which are pre-trained Convolutional Neural Networks. The activations of the fully connected layer "fc6" in AlexNet constitute a $4096-$dimensional feature vector. Similarly, the activations of the fully connected layer "fc6" in VGG-16 constitute another $4096-$dimensional feature vector. The features extracted by both networks are joined together to form a $8192-$dimensional vector. The feature vectors are normalized to have zero-mean and unity-variance along each dimension. The set of

TABLE II
EXPERIMENTAL RESULTS ON FREIBURG GROCERIES DATASET

Method	Accuracy	Time
Proposed (8-bits precision of homomorphic computations)	0.8861	4.9534 s
Proposed (16-bits precision of homomorphic computations)	0.8880	7.9240 s
differentially private distributed deep learning with privacy-loss bound $\epsilon = 0.1$ [29]	0.1356	n/a
differentially private distributed deep learning with privacy-loss bound $\epsilon = 1$ [29]	0.8261	n/a

TABLE III
EXPERIMENTAL RESULTS ON HEART RATE VARIABILITY DATASET

Method	Accuracy	Time
Proposed (8-bits precision of homomorphic computations)	0.8358	3.1571 s
Proposed (16-bits precision of homomorphic computations)	0.9580	4.8610 s
differentially private distributed deep learning with privacy-loss bound $\epsilon = 0.1$ [29]	0.5123	n/a
differentially private distributed deep learning with privacy-loss bound $\epsilon = 1$ [29]	0.6873	n/a

normalized feature vectors is split into a training set containing around 80% of data points and a testing set containing remaining data points. A three-party scenario is created such that Party-A owns all the training data of first ten grocery categories, Party-B owns all the training data of second ten grocery categories, and Party-C owns all the training data of rest five grocery categories. Table II reports the experimental results.

D. A Biomedical Application

As an application example, the mental stress detection problem is considered. The dataset from [25], consisting of heart rate interval measurements of different subjects, is considered for the study of individual stress detection problem. The problem is concerned with the detection of stress on an individual based on the analysis of recorded sequence of R-R intervals, $\{RR^i\}_i$. The R-R data vector at $i-$th time-index, y^i, is defined as $y^i = \begin{bmatrix} RR^i & RR^{i-1} & \cdots & RR^{i-d} \end{bmatrix}^T$. That is, the current interval and history of previous d intervals constitute the data vector. Assuming an average heartbeat of 72 beats per minute, d is chosen as equal to $72 \times 3 = 216$ so that R-R data vector consists of on an average 3-minutes long R-R intervals sequence. A dataset, say $\{y^i\}_i$, is built via 1) preprocessing the R-R interval sequence $\{RR^i\}_i$ with an impulse rejection filter for artifacts detection, and 2) excluding the R-R data vectors containing artifacts from the dataset. The dataset contains the stress-score on a scale from 0 to 100. A label of either "*no-stress*" or "*under-stress*" is assigned to each y^i based on the stress-score. Thus, we have a binary classification problem. A two-party collaborative learning scenario is considered where a randomly chosen subject is considered as Party-A. While keeping Party-A fixed, the distributed learning experiments are performed independently on every other subject being considered as Party-B. For each subject, 50% of the data samples serve as training data while remaining as test data. The subjects, with data containing both the classes and at least 60 samples, are considered for experimentation. There are in total 48 such subjects. The experimental results, averaged over 48 independent experiments, are reported in Table III.

E. Scalability

The computational time required for the homomorphic evaluation of global model depends on the number of parties (i.e. K) participating in collaborative learning. Therefore,
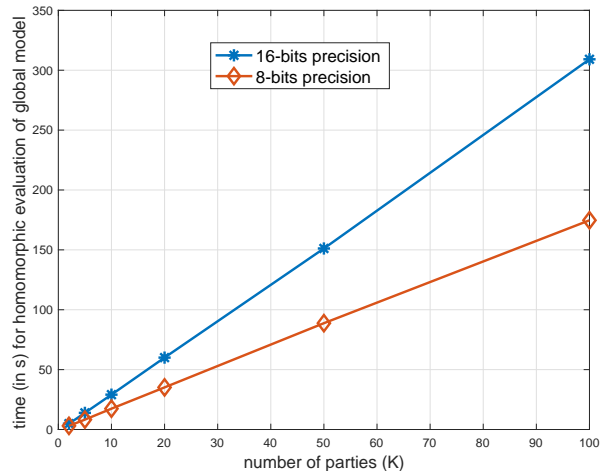

Fig. 3. Computational time vs. number of parties.

experiments are performed to study the computational time as the number of parties is varied from $K = 2$ to $K = 100$. Fig. 3 plots the computational time required for secure homomorphic computations on a MacBook Pro machine with a 2.2 GHz Intel Core i7 processor and 16 GB of memory without using parallel computing. The ratio of computational time to the number of parties is observed to be approximately equal to 3 s for 16-bit precision and 1.75 s for 8-bit precision.

F. Evaluation of the Proposed Approach

To evaluate the gains achieved in accuracy and computational time as a result of the proposed approach to secure distributed deep learning (summarized in Fig. 2), a comparison is made with a variant of the TFHE fully homomorphic encryption scheme [31]. The study in [31] reports the experiments on MNIST dataset for evaluating the neural networks with different depths (referred to as NN-20, NN-50, and NN-100) over TFHE fully homomorphically encrypted data. The results of [31] are compared with the proposed method (considering two-party scenario with Party-A owning odd-digit images and Party-B owning even-digit images) in Table IV.

G. Main Results

Following inferences are made from the results of aforementioned experiments.

TABLE IV
GAINS ACHIEVED BY THE PROPOSED APPROACH ON MNIST DATASET

Method	Security	Machine	Accuracy	Time
Proposed	128-bits	2.2 GHz Intel Core i7	0.987	4.98 s
NN-20 [31]	128-bits	2.6 GHz Intel Core i7	0.971	115.52 s
NN-50 [31]	128-bits	2.6 GHz Intel Core i7	0.947	233.55 s
NN-100 [31]	128-bits	2.6 GHz Intel Core i7	0.830	481.61 s

- As expected, the proposed approach leads to better accuracy (observed in Tables I, II, III) than the differentially private approach [29], since differential privacy requires contaminating data with noise to preserve privacy.
- The proposed membership-mappings based approach is capable of handling the large computational overhead issue of fully homomorphic encryption, since the computational time on a MacBook Pro machine with a 2.2 GHz Intel Core i7 processor and 16 GB of memory (as reported in Tables I, II, III, IV) is practical.
- A linear increase of the computational time with increasing number of parties, as observed in Fig. 3, indicates that the proposed approach is scalable using parallel computing.
- Remarkably, the computational time required for secure homomorphic evaluation of the global model in the cloud is independent of the dimension of the input data, and thus the approach is practical. The computational time depends only on the number of parties and the chosen precision. The ratio of computational time to the number of parties as approximately equal to 3 s for 16-bit precision verifies the application potential.

VII. CONCLUDING REMARKS

This study has outlined a membership-mappings based approach to secure distributed deep learning. The crux of our methodology lies in defining fuzzy attributes (which are induced by globally convergent and robust variational membership-mappings based local deep models) allowing to combine local models by means of a rule-based fuzzy system, thus facilitating the homomorphic evaluation of the global model efficiently. The feature, that the computational time for secure homomorphic evaluation of the global model in the cloud is independent of the dimension of input data, adds to the practicality of the approach. The experimental results verify that the proposed method, while preserving the privacy in a distributed learning scenario using fully homomorphic encryption, remains accurate, practical, and scalable.

APPENDIX A
MEMBERSHIP-MAPPING OUTPUT ESTIMATION

Using (22) and (23), we have

$$\langle (\mathrm{f}_j)_i \rangle_{\mu_{\mathrm{f}_j;\mathrm{u}_j}} = (K_{\mathrm{xa}} K_{\mathrm{aa}}^{-1} \mathrm{u}_j)_i \qquad (98)$$

$$= G(x^i) K_{\mathrm{aa}}^{-1} \mathrm{u}_j. \qquad (99)$$

Thus,

$$\widehat{\mathcal{F}_j(x^i)} = G(x^i) K_{\mathrm{aa}}^{-1} \langle \mathrm{u}_j \rangle_{\mu_{\mathrm{u}_j}^*}. \qquad (100)$$

Using (36) and (31) in (100), we have

$$\widehat{\mathcal{F}_j(x^i)} = \beta \left(G(x^i) \right) K_{\mathrm{aa}}^{-1} \hat{K}_{\mathrm{u}_j} K_{\mathrm{aa}}^{-1} K_{\mathrm{xa}}^T \mathrm{y}_j. \qquad (101)$$

Substituting $\hat{K}_{\mathrm{u}_j}$ from (30) in (101), we get (41).

APPENDIX B
PROOF OF RESULT 2

The proof is split into three parts.

a) Part 1: Since $K_{\mathrm{aa}} > 0$, there exists the unique square root, $K_{\mathrm{aa}}^{1/2} > 0$. Thus,

$$SV^T K_{\mathrm{aa}}^{-1} VS = \left(K_{\mathrm{aa}}^{-1/2} VS \right)^T \left(K_{\mathrm{aa}}^{-1/2} VS \right) \qquad (102)$$
$$> 0. \qquad (103)$$

Since $\tau > 0$ and $\beta > 0$,

$$\mathrm{min\_eigen} \left(I + \frac{1}{(\tau + \beta^{-1})} SV^T K_{\mathrm{aa}}^{-1} VS \right) > 1 \qquad (104)$$

where "$\mathrm{min\_eigen}(\cdot)$" denotes the minimum eigenvalue. Thus,

$$\mathrm{max\_eigen} \left(\left(I + \frac{1}{(\tau + \beta^{-1})} SV^T K_{\mathrm{aa}}^{-1} VS \right)^{-2} \right) < 1 \qquad (105)$$

where "$\mathrm{max\_eigen}(\cdot)$" denotes the maximum eigenvalue. As a result of (105),

$$\mathcal{R}(\beta^{-1}) < \frac{1}{pN} \sum_{j=1}^{p} (\|b_j^1\|^2 + \|b_j^2\|^2). \qquad (106)$$

As U is orthogonal, it follows from (49) that $\|b_j^1\|^2 + \|b_j^2\|^2 = \|\mathrm{y}_j\|^2$, and thus

$$\mathcal{R}(\beta^{-1}) < \beta^{-1}|_{up}. \qquad (107)$$

It follows immediately from (55) that $\mathcal{R}(\beta^{-1}) > \beta^{-1}|_{low}$. Hence, $\mathcal{R}(\beta^{-1}) \in \left(\beta^{-1}|_{low}, \beta^{-1}|_{up} \right)$.

b) Part 2: The derivative of $\mathcal{R}$ w.r.t. β^{-1} is given as

$$\frac{\mathrm{d}\mathcal{R}(\beta^{-1})}{\mathrm{d}\beta^{-1}} = \qquad (108)$$

$$\frac{2}{pN} \sum_{j=1}^{p} \left\{ (\tau + \beta^{-1})(b_j^1)^T \left((\tau + \beta^{-1})I + SV^T K_{\mathrm{aa}}^{-1} VS \right)^{-2} b_j^1 \right.$$
$$\left. - (\tau + \beta^{-1})^2 (b_j^1)^T \left((\tau + \beta^{-1})I + SV^T K_{\mathrm{aa}}^{-1} VS \right)^{-3} b_j^1 \right\}.$$

Consider

$$(\tau + \beta^{-1})^2 (b_j^1)^T \left((\tau + \beta^{-1})I + SV^T K_{\mathrm{aa}}^{-1} VS \right)^{-3} b_j^1$$
$$\leq (\tau + \beta^{-1})^2 \left\| \left((\tau + \beta^{-1})I + SV^T K_{\mathrm{aa}}^{-1} VS \right)^{-1} \right\|_2 \qquad (109)$$
$$\times (b_j^1)^T \left((\tau + \beta^{-1})I + SV^T K_{\mathrm{aa}}^{-1} VS \right)^{-2} b_j^1$$
$$= (\tau + \beta^{-1}) \left\| \left(I + \frac{1}{(\tau + \beta^{-1})} SV^T K_{\mathrm{aa}}^{-1} VS \right)^{-1} \right\|_2 \qquad (110)$$
$$\times (b_j^1)^T \left((\tau + \beta^{-1})I + SV^T K_{\mathrm{aa}}^{-1} VS \right)^{-2} b_j^1$$
$$= (\tau + \beta^{-1}) \frac{(b_j^1)^T \left((\tau + \beta^{-1})I + SV^T K_{\mathrm{aa}}^{-1} VS \right)^{-2} b_j^1}{\mathrm{min\_sing} \left(I + \frac{1}{(\tau+\beta^{-1})} SV^T K_{\mathrm{aa}}^{-1} VS \right)} \qquad (111)$$

where "min_sing($\cdot$)" denotes the minimum singular value. Observing that $\tau > 0$, $\beta^{-1} > 0$, and $SV^T K_{\mathrm{aa}}^{-1} V S > 0$ (i.e. (103)), we have

$$\mathrm{min\_sing}\left(I + \frac{1}{(\tau + \beta^{-1})} SV^T K_{\mathrm{aa}}^{-1} V S\right)$$
$$= 1 + \mathrm{min\_sing}\left(\frac{1}{(\tau + \beta^{-1})} SV^T K_{\mathrm{aa}}^{-1} V S\right)$$
$$> 1. \tag{112}$$

Combining (112) and (111), we have

$$(\tau + \beta^{-1})^2 (b_j^1)^T \left((\tau + \beta^{-1})I + SV^T K_{\mathrm{aa}}^{-1} V S\right)^{-3} b_j^1 \tag{113}$$
$$< (\tau + \beta^{-1})(b_j^1)^T \left((\tau + \beta^{-1})I + SV^T K_{\mathrm{aa}}^{-1} V S\right)^{-2} b_j^1.$$

Using (113) in (108), we get

$$\frac{\mathrm{d}\mathcal{R}(\beta^{-1})}{\mathrm{d}\beta^{-1}} > 0. \tag{114}$$

Observing that $\tau > 0$, $\beta^{-1} > 0$, and $SV^T K_{\mathrm{aa}}^{-1} V S > 0$ (i.e. (103)), we also have

$$(\tau + \beta^{-1})^2 (b_j^1)^T \left((\tau + \beta^{-1})I + SV^T K_{\mathrm{aa}}^{-1} V S\right)^{-3} b_j^1 > 0. \tag{115}$$

Using (115) in (108), we get

$$\frac{\mathrm{d}\mathcal{R}(\beta^{-1})}{\mathrm{d}\beta^{-1}} < \tag{116}$$
$$\frac{2}{pN}(\tau + \beta^{-1}) \sum_{j=1}^{p} (b_j^1)^T \left((\tau + \beta^{-1})I + SV^T K_{\mathrm{aa}}^{-1} V S\right)^{-2} b_j^1.$$

Inequality (116), using (55), can be expressed as

$$\frac{\mathrm{d}\mathcal{R}(\beta^{-1})}{\mathrm{d}\beta^{-1}} < \frac{2}{pN} \frac{pN\mathcal{R}(\beta^{-1}) - \sum_{j=1}^{p} \|b_j^2\|^2}{\tau + \beta^{-1}} \tag{117}$$
$$< \frac{2}{pN} \frac{\sum_{j=1}^{p} \|b_j^1\|^2}{\tau + \beta^{-1}}, \tag{118}$$

where (118) follows using (106). Inequalities (114) and (117) lead to (58).

c) Part 3: Introduce $h(\beta^{-1}) = \mathcal{R}(\beta^{-1}) - \beta^{-1}$, and observe that $h(\beta^{-1}|_{low}) > 0$ and $h(\beta^{-1}|_{up}) < 0$. By the intermediate value theorem, there is a $\hat{\beta}^{-1} \in \left(\beta^{-1}|_{low}, \beta^{-1}|_{up}\right)$ such that $h(\hat{\beta}^{-1}) = 0$, i.e., $\hat{\beta}^{-1} = \mathcal{R}(\hat{\beta}^{-1})$. Thus, $\hat{\beta}^{-1}$ is a fixed point of $\mathcal{R}(\beta^{-1})$.

APPENDIX C
PROOF OF RESULT 3

As $\beta^{-1}|_{it} > \beta^{-1}|_{low}$, it follows from (59) that

$$\tau + \beta^{-1}|_{it} > \frac{2}{pN} \sum_{j=1}^{p} \|y_j\|^2, \tag{119}$$

and thus

$$\frac{\mathrm{d}\mathcal{R}(\beta^{-1}|_{it})}{\mathrm{d}\beta^{-1}} < \frac{\sum_{j=1}^{p} \|b_j^1\|^2}{\sum_{j=1}^{p} \|y_j\|^2} = \frac{\sum_{j=1}^{p} \|b_j^1\|^2}{\sum_{j=1}^{p} (\|b_j^1\|^2 + \|b_j^2\|^2)}. \tag{120}$$

That is, there exists a constant k such that

$$0 < \frac{\mathrm{d}\mathcal{R}(\beta^{-1}|_{it})}{\mathrm{d}\beta^{-1}} \le k < 1, \ \forall it \in \{0, 1, 2, \cdots\}. \tag{121}$$

Let $\hat{\beta}^{-1}$ be a fixed point of $\mathcal{R}(\beta^{-1})$. Now, consider

$$\left|\beta^{-1}|_{it} - \hat{\beta}^{-1}\right| = \left|\mathcal{R}(\beta^{-1}|_{it-1}) - \mathcal{R}(\hat{\beta}^{-1})\right| \tag{122}$$
$$\le k \left|\beta^{-1}|_{it-1} - \hat{\beta}^{-1}\right| \tag{123}$$
$$\vdots \tag{124}$$
$$\le k^{it} \left|\beta^{-1}|_0 - \hat{\beta}^{-1}\right|, \tag{125}$$

that leads to

$$\lim_{it \to \infty} \left|\beta^{-1}|_{it} - \hat{\beta}^{-1}\right| \le \lim_{it \to \infty} k^{it} \left|\beta^{-1}|_0 - \hat{\beta}^{-1}\right| = 0. \tag{126}$$

The uniqueness of the fixed point can be seen via assuming by contradiction that there exists another fixed point, say $\tilde{\beta}^{-1}$. Now consider

$$\left|\tilde{\beta}^{-1} - \hat{\beta}^{-1}\right| = \left|\mathcal{R}(\tilde{\beta}^{-1}) - \mathcal{R}(\hat{\beta}^{-1})\right| \le k \left|\tilde{\beta}^{-1} - \hat{\beta}^{-1}\right| \tag{127}$$
$$< \left|\tilde{\beta}^{-1} - \hat{\beta}^{-1}\right|. \tag{128}$$

This implies that $\tilde{\beta}^{-1} = \hat{\beta}^{-1}$. Hence, the result follows.

APPENDIX D
PROOF OF RESULT 4

According to the triangle inequality,

$$\left\|(K_{\mathrm{xa}} + \Delta_x K_{\mathrm{aa}}^{1/2})\alpha_j^* - (y_j + \Delta y_j)\right\|$$
$$\le \left\|K_{\mathrm{xa}}\alpha_j^* - y_j\right\| + \left\|\Delta_x K_{\mathrm{aa}}^{1/2}\alpha_j^* - \Delta y_j\right\|$$
$$\le \left\|K_{\mathrm{xa}}\alpha_j^* - y_j\right\| + \|[\Delta_x \ \Delta y_j]\|_F \left\|\begin{bmatrix} K_{\mathrm{aa}}^{1/2}\alpha_j^* \\ -1 \end{bmatrix}\right\|$$
$$\le \left\|K_{\mathrm{xa}}\alpha_j^* - y_j\right\| + \delta_m \sqrt{1 + (\alpha_j^*)^T K_{\mathrm{aa}} \alpha_j^*}, \tag{129}$$

and hence

$$\hat{\alpha}_j = \left(K_{\mathrm{xa}}^T K_{\mathrm{xa}} + \delta_m \frac{\|K_{\mathrm{xa}}\hat{\alpha}_j - y_j\|}{\sqrt{1 + \hat{\alpha}_j^T K_{\mathrm{aa}} \hat{\alpha}_j}} K_{\mathrm{aa}}\right)^{-1} K_{\mathrm{xa}}^T y_j. \tag{130}$$

Algorithm 1 estimates $\alpha_j(\hat{\beta}^{-1})$ using (43). It can be seen using (43) that

$$(\tau + \hat{\beta}^{-1}) \frac{\sqrt{1 + (\alpha_j(\hat{\beta}^{-1}))^T K_{\mathrm{aa}} \alpha_j(\hat{\beta}^{-1})}}{\|K_{\mathrm{xa}}\alpha_j(\hat{\beta}^{-1}) - y_j\|} = \delta_m. \tag{131}$$

As a result of (131), it follows from (43) that

$$\alpha_j(\hat{\beta}^{-1}) = \left(K_{\mathrm{xa}}^T K_{\mathrm{xa}} \right. \tag{132}$$
$$\left. + \delta_m \frac{\|K_{\mathrm{xa}}\alpha_j(\hat{\beta}^{-1}) - y_j\|}{\sqrt{1 + (\alpha_j(\hat{\beta}^{-1}))^T K_{\mathrm{aa}} \alpha_j(\hat{\beta}^{-1})}} K_{\mathrm{aa}}\right)^{-1} K_{\mathrm{xa}}^T y_j.$$

As equalities (132) and (130) are identical, $\alpha_j(\hat{\beta}^{-1})$ (which is the solution of (132)) must be equal to $\hat{\alpha}_j$ (which is the solution of (130)), i.e.,

$$\alpha_j(\hat{\beta}^{-1}) = \hat{\alpha}_j. \tag{133}$$

Hence, Algorithm 1 solves the min-max problem (78).

REFERENCES

[1] C. Gentry, "Fully homomorphic encryption using ideal lattices," ser. STOC '09. New York, NY, USA: Association for Computing Machinery, 2009, pp. 169–178.

[2] M. van Dijk, C. Gentry, S. Halevi, and V. Vaikuntanathan, "Fully homomorphic encryption over the integers," in *Advances in Cryptology – EUROCRYPT 2010*, H. Gilbert, Ed. Berlin, Heidelberg: Springer Berlin Heidelberg, 2010, pp. 24–43.

[3] J.-S. Coron, A. Mandal, D. Naccache, and M. Tibouchi, "Fully homomorphic encryption over the integers with shorter public keys," in *Advances in Cryptology – CRYPTO 2011*, P. Rogaway, Ed. Berlin, Heidelberg: Springer Berlin Heidelberg, 2011, pp. 487–504.

[4] J. H. Cheon, J.-S. Coron, J. Kim, M. S. Lee, T. Lepoint, M. Tibouchi, and A. Yun, "Batch fully homomorphic encryption over the integers," in *Advances in Cryptology – EUROCRYPT 2013*, T. Johansson and P. Q. Nguyen, Eds. Berlin, Heidelberg: Springer Berlin Heidelberg, 2013, pp. 315–335.

[5] K. Nuida and K. Kurosawa, "(batch) fully homomorphic encryption over integers for non-binary message spaces," in *Advances in Cryptology – EUROCRYPT 2015*, E. Oswald and M. Fischlin, Eds. Berlin, Heidelberg: Springer Berlin Heidelberg, 2015, pp. 537–555.

[6] O. Regev, "On lattices, learning with errors, random linear codes, and cryptography," in *Proceedings of the Thirty-Seventh Annual ACM Symposium on Theory of Computing*, ser. STOC '05. New York, NY, USA: Association for Computing Machinery, 2005, pp. 84–93.

[7] Z. Brakerski and V. Vaikuntanathan, "Efficient fully homomorphic encryption from (standard) lwe," in *2011 IEEE 52nd Annual Symposium on Foundations of Computer Science*, 2011, pp. 97–106.

[8] Z. Brakerski, C. Gentry, and V. Vaikuntanathan, "(leveled) fully homomorphic encryption without bootstrapping," in *Proceedings of the 3rd Innovations in Theoretical Computer Science Conference*, ser. ITCS '12. New York, NY, USA: Association for Computing Machinery, 2012, pp. 309–325.

[9] Z. Brakerski, "Fully homomorphic encryption without modulus switching from classical gapsvp," in *Advances in Cryptology – CRYPTO 2012*, R. Safavi-Naini and R. Canetti, Eds. Berlin, Heidelberg: Springer Berlin Heidelberg, 2012, pp. 868–886.

[10] J. Fan and F. Vercauteren, "Somewhat practical fully homomorphic encryption," *IACR Cryptol. ePrint Arch.*, vol. 2012, p. 144, 2012. [Online]. Available: http://eprint.iacr.org/2012/144

[11] C. Gentry, A. Sahai, and B. Waters, "Homomorphic encryption from learning with errors: Conceptually-simpler, asymptotically-faster, attribute-based," in *Advances in Cryptology – CRYPTO 2013*, R. Canetti and J. A. Garay, Eds. Berlin, Heidelberg: Springer Berlin Heidelberg, 2013, pp. 75–92.

[12] L. Ducas and D. Micciancio, "Fhew: Bootstrapping homomorphic encryption in less than a second," in *Advances in Cryptology – EUROCRYPT 2015*, E. Oswald and M. Fischlin, Eds. Berlin, Heidelberg: Springer Berlin Heidelberg, 2015, pp. 617–640.

[13] I. Chillotti, N. Gama, M. Georgieva, and M. Izabachène, "Faster fully homomorphic encryption: Bootstrapping in less than 0.1 seconds," in *Advances in Cryptology – ASIACRYPT 2016*, J. H. Cheon and T. Takagi, Eds. Berlin, Heidelberg: Springer Berlin Heidelberg, 2016, pp. 3–33.

[14] ——, "Faster packed homomorphic operations and efficient circuit bootstrapping for tfhe," in *Advances in Cryptology – ASIACRYPT 2017*, T. Takagi and T. Peyrin, Eds. Cham: Springer International Publishing, 2017, pp. 377–408.

[15] ——, "TFHE: Fast fully homomorphic encryption library," August 2016, https://tfhe.github.io/tfhe/.

[16] S. Park, S. J. Lee, E. Weiss, and Y. Motai, "Intra- and inter-fractional variation prediction of lung tumors using fuzzy deep learning," *IEEE Journal of Translational Engineering in Health and Medicine*, vol. 4, pp. 1–12, 2016.

[17] Y. Deng, Z. Ren, Y. Kong, F. Bao, and Q. Dai, "A hierarchical fused fuzzy deep neural network for data classification," *IEEE Transactions on Fuzzy Systems*, vol. 25, no. 4, pp. 1006–1012, Aug 2017.

[18] S. Zhou, Q. Chen, and X. Wang, "Fuzzy deep belief networks for semi-supervised sentiment classification," *Neurocomput.*, vol. 131, pp. 312–322, May 2014.

[19] C. E. Hatri and J. Boumhidi, "Fuzzy deep learning based urban traffic incident detection," in *2017 Intelligent Systems and Computer Vision (ISCV)*, April 2017, pp. 1–6.

[20] D. Bonanno, K. Nock, L. Smith, P. Elmore, and F. Petry, "An approach to explainable deep learning using fuzzy inference," in *Proc. SPIE 10207, Next-Generation Analyst V, 102070D*, May 2017.

[21] Z. Jiang, S. Gao, and M. Li, "An improved advertising ctr prediction approach based on the fuzzy deep neural network," *PLOS ONE*, vol. 13, no. 5, pp. 1–24, 05 2018. [Online]. Available: https://doi.org/10.1371/journal.pone.0190831

[22] R. Zhang, F. Shen, and J. Zhao, "A model with fuzzy granulation and deep belief networks for exchange rate forecasting," in *2014 International Joint Conference on Neural Networks (IJCNN)*, 2014, pp. 366–373.

[23] M. Wang, Z.-H. Ning, T. Li, and C.-B. Xiao, "Information geometry enhanced fuzzy deep belief networks for sentiment classification," *International Journal of Machine Learning and Cybernetics*, vol. 10, no. 11, pp. 3031–3042, 2019.

[24] M. Kumar and B. Freudenthaler, "Fuzzy membership functional analysis for nonparametric deep models of image features," *IEEE Transactions on Fuzzy Systems*, vol. 28, no. 12, pp. 3345–3359, 2020.

[25] M. Kumar, W. Zhang, M. Weippert, and B. Freudenthaler, "An explainable fuzzy theoretic nonparametric deep model for stress assessment using heartbeat intervals analysis," *IEEE Transactions on Fuzzy Systems*, pp. 1–1, 2020.

[26] M. Kumar, S. Singh, and B. Freudenthaler, "Gaussian fuzzy theoretic analysis for variational learning of nested compositions," *International Journal of Approximate Reasoning*, vol. 131, pp. 1–29, 2021.

[27] M. Kumar, B. Moser, L. Fischer, and B. Freudenthaler, "Membership-mappings for data representation learning: Measure theoretic conceptualization," in *Database and Expert Systems Applications - DEXA 2021 Workshops*, G. Kotsis, A. M. Tjoa, I. Khalil, B. Moser, A. Mashkoor, J. Sametinger, A. Fensel, J. Martinez-Gil, L. Fischer, G. Czech, F. Sobieczky, and S. Khan, Eds. Cham: Springer International Publishing, 2021, pp. 127–137.

[28] ——, "Membership-mappings for data representation learning: A bregman divergence based conditionally deep autoencoder," in *Database and Expert Systems Applications - DEXA 2021 Workshops*, G. Kotsis, A. M. Tjoa, I. Khalil, B. Moser, A. Mashkoor, J. Sametinger, A. Fensel, J. Martinez-Gil, L. Fischer, G. Czech, F. Sobieczky, and S. Khan, Eds. Cham: Springer International Publishing, 2021, pp. 138–147.

[29] M. Kumar, M. Rossbory, B. A. Moser, and B. Freudenthaler, "An optimal $(\epsilon, \delta)-$differentially private learning of distributed deep fuzzy models," *Information Sciences*, vol. 546, pp. 87–120, 2021.

[30] ——, "Differentially private learning of distributed deep models," in *Adjunct Publication of the 28th ACM Conference on User Modeling, Adaptation and Personalization*, ser. UMAP '20 Adjunct. New York, NY, USA: Association for Computing Machinery, 2020, pp. 193–200.

[31] I. Chillotti, M. Joye, and P. Paillier, "Programmable bootstrapping enables efficient homomorphic inference of deep neural networks," in *Cyber Security Cryptography and Machine Learning - 5th International Symposium, CSCML 2021, Be'er Sheva, Israel, July 8-9, 2021, Proceedings*, ser. Lecture Notes in Computer Science, S. Dolev, O. Margalit, B. Pinkas, and A. A. Schwarzmann, Eds., vol. 12716. Springer, 2021, pp. 1–19. [Online]. Available: https://doi.org/10.1007/978-3-030-78086-9_1